Universidade de Lisboa

Faculdade de Farmácia

PROIMMUNOTOXIN: A NOVEL DESIGN STRATEGY OF IMMUNOTOXINS APPLIED TO BREAST CANCER

Ana Margarida de Abreu Manuel

Dissertation supervised by Professor Doctor João Gonçalves.

Biopharmaceutical Sciences Master

2018

Abbreviations

ADCC	Antibody-dependent cell-mediated cytotoxicity
Akt	Ak transforming factor
Amp	Ampicillin
Bp	Base pair
BSA	Bovine Serum Albumin
CD16	Cluster of differentiation 16
DMEM	Dulbecco's Modified Eagle's Medium
DMSO	Dimethyl Sulfoxide
DNA	Deoxyribonucleic Acid
dsFv	Disulfide-stabilized variable fragment
DT	Diphtheria toxin
eEF-1	Eukaryotic Elongation Factor 1
eEF-2	Eukaryotic Elongation Factor 2
EGFR	Epidermal Growth Factor Receptor
ELISA	Enzyme-Linked Immunosorbent Assay
ER	Endoplasmic reticulum
Fab	Antigen-binding fragment
FBS	Fetal Bovine Serum
FITC	Fluorescein isothiocyanate
Fc	Fragment crystallizable
Fv	Variable fragment
kDa	Weight unit - kilodalton (s)
g	Weight unit - gram (s)
g	Acceleration unit - gravitational force
h	Time unit - hour (s)
HEK 293T	Human Embryonic Kidney 293T cells
HER1	Receptor tyrosine-protein kinase erbB-1
HER2	Receptor tyrosine-protein kinase erbB-2
HR	Hormone receptors
IgG1	Immunoglobulin G1
IT	Immunotoxin
LB	Luria-Bertani broth
M	Matter unit - molar

mAbs	Monoclonal antibodies
MAPK	Mitogen-activated protein kinase
mg	Weight unit - milligram (s)
min	Time unit - minute (s)
mL	Volume unit - millilitre
mM	Matter unit - milimolar
MTT	Methylthiazolyldiphenyl-tetrazolium bromide
m/v	Concentration unit - weight/volume
PBS	Phosphate Buffered Saline
PBS-T	Phosphate Buffered Saline-Tween
PE	Pseudomonas exotoxin
PEI	Polyethylenimine
PIT	Proimmunotoxin
PMSA	Prostate-specific membrane antigen
PSA	Penicillin-Streptomycin-Amphotericin B
RIPA	Radio-Immunoprecipitation assay
RNA	Ribonucleic Acid
rpm	Rotations per minute
rRNA	Ribosomal Ribonucleic Acid
RT-PCR	Real Time – Polymerase Chain Reaction
scFv	Single chain variable fragment
SPR	Surface Plasmon resonance
TBS-T	Tris Buffered Saline-Tween
VH	Variable domain of the heavy chain
VHH	Variable domain of camelid heavy chain antibody
VL	Variable domain of the light chain
v/v	Concentration unit - volume/volume
µL	Volume unit - microliter (s)

Abstract

Breast cancer is the second leading cause of death among female cancer patients. One of the most used therapies against receptor tyrosine-protein kinase erbB-2 (HER2)$^{+}$ metastatic breast cancer is the monoclonal antibody Trastuzumab. This antibody can be used in therapy either alone or in conjugation with chemotherapeutics. Though it has shown to lead to an increase in patient's overall survival, this therapy may also lead to the acquirement of resistance in patients with prolonged usage.

Immunotoxins have been pursued for a long time as a new and innovative type of biopharmaceutical against cancer because they combine the cytotoxicity of a variety of toxins with the specificity of antibodies. An immunotoxin combining Ricin A-chain [Ricin A] and an antibody targeting breast cancer has already been tried as a therapeutic. However, the observed non-specific toxicity prevented further studies. To address the problem of non-specific toxicity observed in immunotoxins, one possible solution could be the neutralization of the active toxin during blood circulation. Recently, variable domain from alpacas heavy chain antibody (VHH), targeting Ricin A, have been described to effectively neutralize Ricin toxin *in vitro* and to protect mice from Ricin toxicity *in vivo*.

Taking in consideration these concepts, a new type of immunotoxin could be envisioned. A proimmunotoxin which comprises Trastuzumab linked to a Ricin A neutralizing VHH, may be capable of delivering Ricin A toxin with high specificity to HER2^{+} breast cancer cells, while neutralizing its activity during blood circulation, overcoming the non-specific toxic side effects of a normal immunotoxin and resistance to Trastuzumab. The results here presented show that this new type of immunotoxin retains the specificity of the antibody Trastuzumab towards HER2, shows affinity towards Ricin A, and most importantly, it can protect HER2^{-} cells, while retaining the ability to deliver Ricin A toxin to HER2^{+} breast cancer cells, decreasing cell viability. The possibility of clustering HER2 at the cell membrane to enhance the internalization and trafficking of the proimmunotoxin was also studied by constructing one with two different binding sites to HER2. Preliminary results show that this proimmunotoxin has a quicker internalization by the cells, shown by an enhanced decrease in cell viability.

Keywords: Breast cancer; HER2; Trastuzumab; immunotoxin; Ricin A.

Resumo

De acordo com a *American Cancer Society,* é estimado que o cancro da mama provoque aproximadamente 40,920 mortes em 2018, apenas nos Estados Unidos da América. Este tipo de cancro é a segunda maior causa de morte entre mulheres diagnosticadas com cancro, mas pode também afetar homens. A doença pode ser classificada em diversos subtipos, sendo que o cancro da mama HER2$^+$ afeta entre 20% a 30% das mulheres que sofrem desta doença. Este é caracterizado pela sobrexpressão ou amplificação do gene *c-erbB-2*, que codifica para o recetor tipo 2 do fator de crescimento epidérmico humano, cuja função principal é a regulação do crescimento celular. A sobrexpressão de HER2 leva a um crescimento celular descontrolado que aumenta a probabilidade de metastização de células cancerígenas, aumentando a taxa de mortalidade e levando a um pior prognóstico dos doentes diagnosticados com cancro da mama HER2$^+$.

A terapia mais recorrente em doentes com cancro da mama HER2$^+$ é o anticorpo monoclonal Trastuzumab, sendo que esta terapia pode ser feita com ou sem a administração de outros fármacos. Este anticorpo exerce o seu efeito terapêutico ligando-se ao recetor HER2 impedindo a transdução de sinal através da via PI3K/Akt e aumentando a sua internalização e possível degradação. Este anticorpo promove também o recrutamento de células imunitárias, como por exemplo as células *Natural Kille*r (NK), através de um mecanismo mediado pelo recetor CD16. O principal problema com a utilização deste tratamento é a necessidade de um uso recorrente do mesmo, o que leva muitas vezes à aquisição de resistência à terapia por parte destes doentes.

De forma a aumentar a citotoxicidade de anticorpos monoclonais utilizados na terapia contra o cancro, tem-se recorrido a técnicas de biologia molecular para combinar anticorpos ou fragmentos dos mesmos com toxinas - estas novas moléculas são denominadas de imunotoxinas. A vantagem destas imunotoxinas na terapêutica contra o cancro é que comparativamente aos anticorpos terapêuticos que as constituem, conseguem promover um aumento da citotoxicidade através da junção de uma grande variedade de toxinas, mantendo a especificidade para os seus alvos terapêuticos, permitindo assim a sua distribuição às células cancerígenas.

De entre as toxinas que podem ser utilizadas para a construção de imunotoxinas, a Ricina, proteína de origem vegetal extraída da planta *Ricinus communis L.*, é uma das que mostra maior relevância devido à sua potente citotoxicidade. Esta proteína é constituída por duas cadeias polipeptídicas, a cadeia A é conhecida pela sua capacidade de depurinação de uma base de adenina na subunidade 28 do RNA ribossomal, causando a inativação dos

ribossomas e consequentemente à paragem da síntese proteica, levando à morte das células por apoptose. Sendo a cadeia A a componente tóxica desta toxina, a cadeia B está encarregue da entrada da toxina na célula, através da sua ligação a resíduos de galactose presentes na superfície das células.

Até hoje já foram testadas várias imunotoxinas que combinam a toxina Ricina com anticorpos que têm como alvo o cancro da mama e, apesar de mostrarem bons resultados iniciais, os efeitos de toxicidade não-específica observados em pacientes após a administração destes biofármacos impedem a sua comercialização. Uma possível solução aos efeitos observados pode passar pela neutralização da toxina ativa durante a sua circulação sanguínea.

A descoberta de anticorpos formados apenas pela sua cadeia pesada em camelídeos revolucionou o conceito de anticorpo monoclonal e permitiu a construção de novos fragmentos de anticorpo, os fragmentos variáveis da cadeia pesada de camelídeos, ou em inglês *variable domain of camelid heavy chain antibody* (VHH). Os VHH além de manterem a especificidade dos anticorpos monoclonais têm como vantagem adicional a sua reduzida dimensão, o que permite um grande número de aplicações que não seriam possíveis com anticorpos monoclonais.

Vance D. J. e os seus colaboradores construíram recentemente monómeros e heterodímeros de VHHs que são capazes de neutralizar eficazmente a Ricina *in vitro* e proteger ratinhos da sua toxicidade *in vivo*, tendo como alvo quer a cadeia A como a cadeia B desta toxina.

Através dos conceitos apresentados acima, é possível idealizar um novo conceito de imunotoxina. Em vez de utilizar a convencional construção de imunotoxina, cujo anticorpo se encontra diretamente ligado à toxina, o anticorpo irá encontrar-se ligado a VHHs anti-toxina que irão não só neutralizar a mesma durante a sua circulação sanguínea, mas também entregar especificamente a toxina às células.

Neste projeto apresentamos um novo conceito de imunotoxina, uma proimunotoxina, que irá fundir o anticorpo Trastuzumab a dois homodímeros VHH anti-Ricina A, que será capaz de entregar a cadeia A da toxina Ricina especificamente a células de cancro da mama HER2$^+$, tentando desta forma evitar os efeitos de toxicidade não específica.

A criação de uma proimunotoxina permitiu em paralelo o estudo de uma construção similar com o objetivo de aumentar a sua internalização através do *clustering* de recetores HER2 à superfície da célula, de forma similar ao que foi feito por Moody, P. R. *et al*.

Inicialmente procedeu-se à construção de dois anticorpos, Tras-VHH-R, constituído pelo anticorpo Trastuzumab em formato scFv-Fc que se encontra ligado pela região Fc a dois homodímeros VHH anti-Ricina A e o anticorpo Tras-VHH-R-H, constituído também pelo anticorpo Trastuzumab no mesmo formato ligado a dois heterodímeros, constituídos por um VHH anti-Ricina A e um VHH anti-HER2, que na presença de Ricina A constituem a proimunotoxina 1 (PIT1) e proimunotoxina 2 (PIT2), respetivamente. Estes anticorpos foram produzidos em células 293-F FreeStyle™ e eficazmente purificados através de cromatografia de afinidade com colunas de Proteína A Sepharose.

A afinidade relativa dos anticorpos Tras-VHH-R e Tras-VHH-R-H para com a cadeia A da toxina Ricina foi estudada utilizando um ensaio de imunoabsorção enzimática (ELISA), revelando baixos valores EC_{50} para ambos os anticorpos demonstrando uma alta afinidade à cadeia A de Ricina, que se deve exclusivamente aos VHHs anti-Ricina A presentes na sua constituição. O estudo da especificidade destes anticorpos para com o recetor HER2 foi estudado através de citometria de fluxo, demonstrando resultados similares entre os anticorpos contruídos neste projeto e o anticorpo Trastuzumab, com valores superiores a 95 % de células marcadas para a linha celular SKBR3 (HER2$^+$) e inferiores a 2 % para a linha celular HeLa P4 (HER2$^-$), para concentrações de anticorpo superiores a 0.8 nM.

Por último, a citotoxicidade das proimunotoxinas foi testada através de um ensaio de MTT (brometo de [3-(4,5-dimetiltiazol-2yl)-2,5-difenil tetrazolium). Células SKBR3 e HeLa P4 foram incubadas com Ricina A, anticorpo (Tras-VHH-R ou Tras-VHH-R-H) e PIT 1 ou 2 a diferentes concentrações separadamente, durante períodos de 48 ou 72 h. Os resultados de viabilidade celular obtidos confirmam a existência de concentrações de PIT 1 e 2 para as quais a viabilidade celular na linha celular SKBR3 é inferior a 60% mantendo a viabilidade celular superior a 90 % na linha celular HeLa P4, demonstrando que as PIT construídas neste projeto são capazes de matar células cancerígenas HER2$^+$, protegendo as células HER2$^-$. Comparando a PIT1 com a PIT2 é possível perceber uma diferença significativa na viabilidade celular entre as duas PIT, sendo que a PIT2 demonstra resultados de viabilidade celular inferiores à PIT1 em diferentes concentrações. Com base nestes resultados preliminares é possível concluir que o *clustering* de recetores HER2 à superfície da célula é capaz aumentar a internalização de proimunotoxinas e possivelmente ajudar no seu tráfico intracelular e por consequência na libertação da toxina dentro da célula. A aplicação deste conceito noutros veículos de transporte biológico de toxinas ou fármacos por anticorpos pode ser muito importante no aumento da sua eficácia e diminuição da sua toxicidade inespecífica.

No futuro esperamos poder continuar com ensaios de internalização celular e microscopia confocal de forma a compreender melhor o modo como estas proimunotoxinas são internalizadas e o seu percurso no interior da célula. Ensaios de morte celular serão posteriormente realizados de forma a perceber quais as vias de morte celular que são ativadas aquando da libertação da toxina. Seria também muito importante começar os estudos em linhas celulares resistentes ao Trastuzumab de forma a poder viabilizar este novo biofármaco ao maior conjunto de pacientes possível.

O que torna este conceito de proimunotoxina tão interessante é a possibilidade de ser aplicado a um grande conjunto de anticorpos e toxinas, mas também ao transporte de fármacos. Desta forma, esperamos que as experiências efetuadas neste trabalho possam contribuir para o avanço da disponibilização de novos e potentes biofármacos contra o cancro da mama.

Acknowledgements

Table of Contents

Figure Index

Figure 5 Transduction by the HER family. There are four members of the HER family: HER1, HER2, HER3, and HER4. There are receptor-specific ligands for HER1, HER3, and HER4. An intracellular tyrosine kinase domain exists for HER1, HER2, and HER4. Phosphorylation of the tyrosine kinase domain by means of homodimerization or heterodimerization induces both cell proliferation and survival signalling. HER2 is the preferred dimerization partner for the other HER family members. The phosphorylated tyrosine residues on the intracellular domain of HER2 activate the lipid kinase phosphoinositide 3-kinase (PI3-K), which phosphorylates a phosphatidylinositol that in turn phosphorylates the enzyme Ak transforming factor (Akt), driving cell survival. In parallel, a guanine nucleotide exchange factor, the mammalian homologue of the son of seven-less (SOS), activates the rat sarcoma

1.   Introduction

The history of immunotoxins (IT) began in the 1970s when many researchers tried to conjugate the specificity of monoclonal antibodies (mAbs) with the potent cytotoxicity of different toxins, hypothesizing that the synergic effect of both molecules could lead to a new and powerful cancer therapy. The turning point of this search was achieved by Thorpe *et al*. when a successful immunotoxin was produced [1]. Since then, the field of immunotoxins has suffered a tremendous transformation, evolving side by side with mAbs and molecular engineering, offering today the chance to produce potent ITs against a vast number of cancers. Until today, only one IT was approved by the FDA (Food and Drug Administration), used for treatment of Cutaneous T-cell Lymphoma (Denileukin Diftitox — trade name Ontak), but several are now in clinical trials waiting for approval [2,3]. Although many difficulties have been overcome through this forty years path, there are still improvements to be made until the perfect immunotoxin construct is achieved.

1.1   Immunotoxin Structure Over Time

An IT has two major components responsible for its main characteristics. The antibody is responsible for the specificity and the cytotoxic protein, here referred as toxin, for killing the target cell. The linkage of these two components can be achieved by different methods: gene fusions, peptide bonds, disulfide bonds, and thioether bonds.

The first generation of ITs was constructed by chemically binding mAbs with whole toxins, as the ones produced by conjugating different mAbs to *Pseudomonas* exotoxin (PE) protein (Figure 1).

The understanding of the structural domains of PE and consequent deletion of its binding domain led to the creation of the second generation of ITs, composed of toxins lacking their receptor-binding domain. However, to preserve essential toxin functions, the variable fragment (Fv) or antigen-binding fragment (Fab) was inserted in the location of the toxin binding domain [4].

With the improvement of molecular cloning techniques, it was then possible to create a new generation of ITs by fusing the modified toxin and antibody fragments genes [5]. The first recombinant antibody-toxin fusion protein was accomplished by Chaudhary and his co-workers, by fusing two Fv with PE [6]. The heavy (VH) and light (VL) variable domains of these ITs can be linked by either a peptide linker (single chain variable fragment - scFv) or a disulphide bond (disulfide-stabilized variable fragment - dsFv).

From the 1st to the 3rd generation of ITs, the main goal was to engineer these molecules to present lower immunogenicity and subsequently use them in clinical cancer therapies. The improvement of the 3rd generation of ITs raised various questions regarding the mechanism by which the toxin was released after internalization and how it was possible to improve those mechanisms.
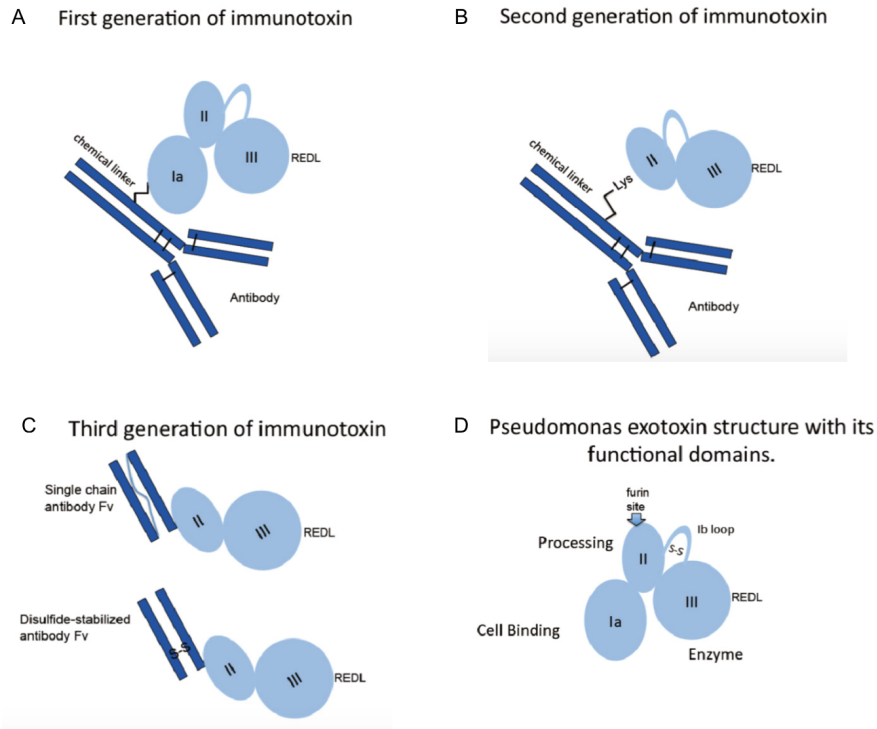
Figure 1 IT constructions from oldest to newest. **A)** First generation ITs were constructed by using chemical crosslinking agents to attach intact toxins to intact antibodies. **B)** Second generation ITs used modified toxins lacking receptor-binding domains. **C)** Third generation molecules used cloned antibody fragments fused to modified toxin genes; allowing for the recombinant production of homogeneous protein. **D)** *Pseudomona*s exotoxin structure. Adapted from Antignani, A. & FitzGerald, D., (2013).

1.2   IT Assembly

1.2.1   Choosing target antigen

Sometimes even the best toxin when conjugated produces side effects that can only be improved with alterations in the antibody and target antigen. Besides, we can have a great toxin but if it is not efficiently internalized it cannot produce its cytotoxic effect. It is well known that there are antigens that more efficiently internalize ITs than others. For example, ITs directed to CD22 are more efficiently internalized and more potent than those to CD19, despite the fact that the number of molecules associated to the cell surface is greater with CD19 [7].

One important step in the design of an IT is choosing the appropriate antigen and respective antibody. The chosen antigen must be tumour-specific or tumour-associated, have high levels of expression on cell surface, be present in a wide range of tumour samples, and the antibody binding to the antigen must produce an efficient IT internalization. Several antigens have been found to have one or two of the previous characteristics but not the whole set. For example, CD33 is found to be expressed in myeloid cells in almost 90 to 95% of all Acute Myeloid Leukaemia patients [8]. However, due to its low expression levels in myeloid cells, this glycoprotein is not considered a suitable target antigen.

Most of target antigens used for treatment with ITs are tumour-associated and not tumour-specific, as they ideally should be. In other words, these antigens are present in both normal and tumour cells. In normal cells they can either be expressed at a minimum level on cell surface or only present in the cytoplasm, whereas in tumour cells they are either overexpressed or they begin to be expressed on cell surface [9]. The prostate-specific membrane antigen (PMSA) and the HER2 are both examples of tumour-associated antigens. PSMA has been used as a target antigen for diverse ITs [10,11], since it is only expressed on cell surface in tumour cells, not posing any threat to normal cells. Regarding HER2 the same does not apply, since HER2 is expressed at the cell surface of both normal and tumour cells. To use this antigen as a target for ITs, an overexpression is needed in tumour cells. This overexpression occurs in various types of breast cancers for which many ITs are produced and used against [12].

1.2.2   Choosing the antibody structure

After choosing the target antigen, the next step in IT design is the engineering of the antibody fragment, which is going to make the connection between the toxin and the antigen, leading the toxin inside the cell for its final purpose.

Through recombinant DNA techniques it is now possible to produce a wide range of antibody fragments from the known structure of the antibody light and heavy chain. The smallest antibody fragment produced until now is the scFv, constructed by VL and VH of a full-length antibody. Although ITs constructed with scFv have a good capacity in penetrating solid tumour masses due to their low molecular weight, they have a lower binding affinity because of the scFv monovalency and, furthermore, they are quickly cleared of the bloodstream, not having the most desirable pharmacokinetics [13].

Pharmacokinetics can be improved by constructing ITs with bivalent scFv (tandem scFv and diabody), scFv-fusion proteins (minibody and scFv-Fc) and bispecific scFv (Figure 2) [14,15].
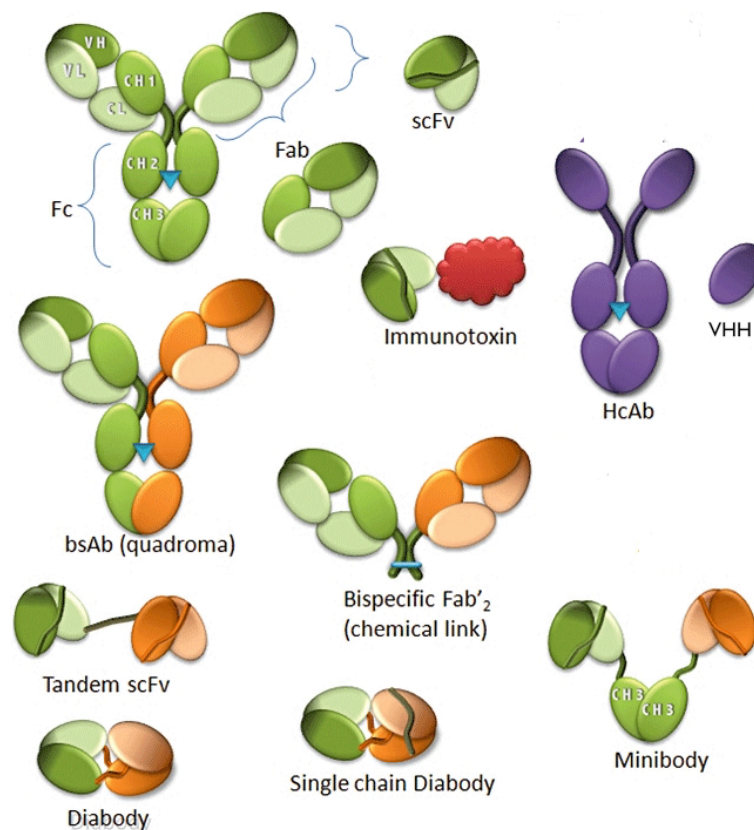
Figure 2 Antibody fragments with therapeutic potential. A conventional antibody is depicted in green (light for light chain, dark for heavy chain, blue triangle indicates the glycosylation site) and the derived fragments (shaded areas represent the binding sites). The orange colour symbolizes a different specificity. HcAb from camelids and their fragments (VHH for single-domain antibodies) are depicted in purple. The red molecule represents the toxin. Adapted from Chames, P. *et al.*, (2009).

Bivalent and bispecific scFv are both engineered by linking two scFv with a peptide linker. The difference being the specificity of the two scFv: bispecific scFv are composed by two different scFv while bivalent scFv are composed by two equal scFv. Thus, bispecific scFv can recognize two different antigens. The peptide linker usually used is rich in serine or threonine for solubility and glycine for flexibility [16]. These two scFv can be constructed in the form of a single peptide chain, with the use of long peptide linker between chains (tandem scFv) or through the use of a short peptide linker ($\approx$ 5 amino acids) between the VH and VL of the same scFv, preventing the dimerization of these two chains, but allowing the VH of one scFv to dimerize with the VL of the other through the use of a long peptide linker ($\approx$ 15 amino acids) (single chain diabody).

Although bivalent scFv take more time to be cleared from the bloodstream it still takes a shorter time compared to antibody drug conjugates (4 to 8 hours more). To solve this problem other antibody fragments have been constructed, such as triabodies, tetrabodies and scFv-Fc.

The most recent strategy in IT design is the use of VHHs. First discovered in camelids, VHHs consist of the single variable heavy domain of camelids [17], which produce antibodies only composed of two heavy chains. VHHs maintain high affinity and specificity, equal to conventional antibodies, retaining the capacity of scFv to penetrate solid tumour masses with low immunogenicity [18]. Making them a desirable approach to IT construction

Despite the fact that there is now a wide variety of antibody fragments that can be used in IT construction, the balance between binding affinity, blood clearance and tumour mass penetration is still difficult to achieve.

1.2.3   Choosing the toxin - Ricin Toxin

When choosing a new toxin to conjugate to antibodies, there are several characteristics that researchers look for before committing to it. It is important to understand the toxin structure and domain orientation, cloning easiness, and, if possible, expression and purification yields [5]. The perfect toxin, when conjugated to an antibody, would be non-immunogenic, non-toxic during blood circulation and still highly potent.

Among the most potent toxins, there is the Ricin toxin, which is a protein toxin derived from the seeds of the castor plant *Ricinus communis*. Ricin is a 64 kDa heterodimeric protein, comprising two polypeptide chains (A ≈ 30 kDa and B ≈ 32 kDa), linked by a disulfide bond [19]. Its cytotoxic capacity comes from the enzymatic activity of its A chain.

The N-glycosylase activity of Ricin A chain allows the inactivation of eukaryotic ribosomes by hydrolysis of the *N*-glycosylic bond of a single adenine in position 4324 of the 28S rRNA at 60S ribosomal subunit, which is extremely important in the elongation process of the polypeptide chain [20]. Without this adenine, the eukaryotic elongation factor 1 (eEF-1) and 2 (eEF-2) cannot bind to the ribosome, ceasing protein synthesis and thus initiating the apoptotic process in the cell [21]. The B chain serves a completely different purpose, being responsible for the delivery of the A-B complex to the cell. It is a lectin that binds to cell surface glycolipids and glycoproteins that possess β-(1→4)-linked galactose residues [22]. Due to the existence of several cell surface receptors with this type of residues, B chain binding can mediate an endocytic mechanism, leading to Ricin internalization.

After internalization, approximately 5% of internalized Ricin is transported from early endosomes to the Golgi complex. From this complex the Ricin toxin is then transported retrogradely to the Endoplasmic Reticulum (ER), where the internal disulphide bond connecting the A and B chain is reduced, and the A chain can then escape to the cytosol [23,24]. The mechanism by which the A chain escapes the ER is still poorly understood, but once in the cytosol, the A chain can arrest protein synthesis and lead to apoptosis by a series of different mechanisms. It can either activate the extrinsic pathway of apoptosis, involving caspase 8 and 10, or the intrinsic or mitochondrial pathway, involving caspase 9 as the initiator caspase. Both these pathways can lead to the cleavage of effector caspases such as caspase 3. It is reported that Ricin leads to apoptosis mainly by activation of the mitochondrial pathway due to the loss in mitochondrial membrane potential, release of cytochrome *c* and cleavage of caspase 9 and 3 but not caspase 8 [25–28].
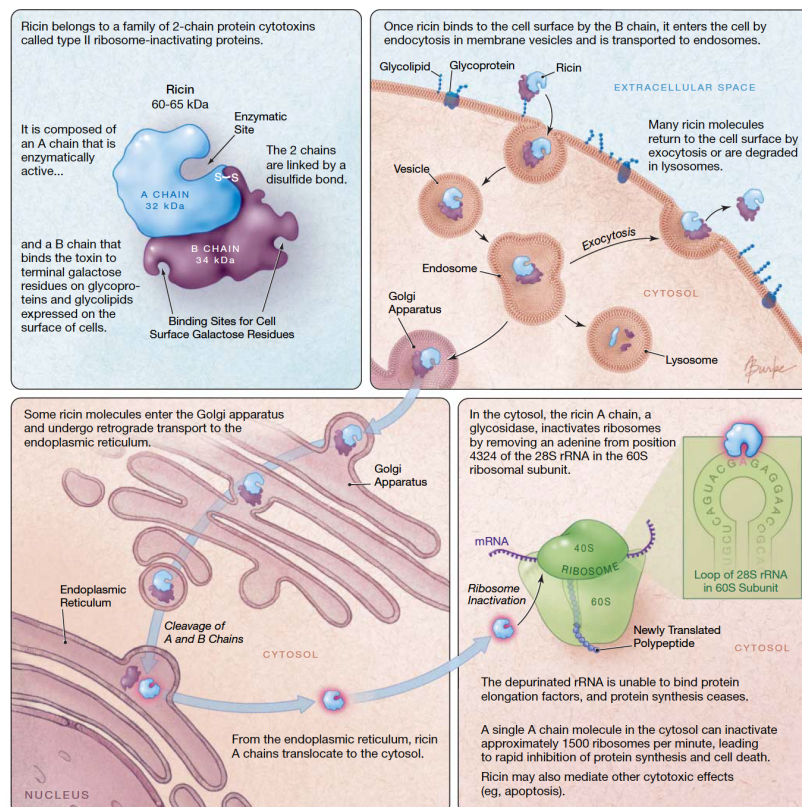
Figure 3 Mechanism of Ricin toxicity. Adapted from Audi, J. *et al.*, (2005).

The anti-p185[HER-2]-RTA IT is the example of a chemically conjugated anti-HER2 mAb with Ricin A chain, that was able to inhibit cell growth and activate the apoptotic cascade through the cleavage of caspase 9 and subsequently caspase 3 [29]. Although many of these ITs showed promising *in vitro* results their side-effects have prevented the use in clinical development.

1.3   The Toxin Journey Inside the Cell

In order to kill the target cell, the toxin must reach the cytosol, since many of them act on protein synthesis. Therefore, the uncoupling of the toxin from the antibody is an important step and can be accomplished by different ways: protease degradation, more common due to the majority of ITs being produced by molecular engineering; disulfide bond reduction; or hydrolysis of an acid-labile bond in exposure to an acidic environment.

Although many ITs are now produced through the use of a peptide linker, there are still ITs that impose some difficulties in being constructed by this technique and still require linkage through disulfide or acid-labile bond. This is the case of the Ricin-based ITs, due to a difficulty in producing functional gene fusions [4].

After being internalized, the IT is entrapped in an endosome that will, under normal conditions, be transformed into a lysosome. Unlike many antibody-drug conjugates, of which the drug can resist low pHs [30], protein toxins must escape lysosomal degradation to stay intact and maintain their enzymatic activity [31].

ITs constructed by molecular engineering escape the endosomes and are released from the antibody like it would normally occur when they were toxins comprising their binding domain.

For ITs constructed with the diphtheria toxin (DT) or PE, toxin release is dependent on a furin-like cleavage followed by the reduction of a key disulfide bond [32,33]. PE and DT both halt protein synthesis at the elongation step, killing by similar mechanisms [34]. In the endosomes, after the furin cleavage of PE, the protein is transported through the Golgi complex to the ER where it adenosine diphosphate (ADP)-ribosylates the eEF-2 (Figure 4). Although the way by which PE escapes the ER is unknown [2], it is known that the traffic to ER requires KDEL-like sequence [4].

There are also toxins that halt protein synthesis by using different mechanisms, for example the plant toxin Ricin. As mentioned before, this toxin depurinates an important adenine in 28S ribosomal ribonucleic acid (rRNA), inactivating the ribosome [35]. The modifications produced by these toxins simulate the apoptotic pathway leading to cell death. Despite the fact that the release of Ricin from the antibody is different from PE, the journey of these two proteins to the cytosol is very similar [20,36] (Figure 4).

Although early studies have demonstrated that only one molecule in a million internalized gelonin IT molecules reach the cytosol [37], and for PE only 4% of cell-associated toxin molecules reach the cytosol [38], it is known that for some protein toxins only one internalized molecule is necessary to have cell death [39]. By choosing the best antibody and

antigen for the target cell, toxin internalization can be improved. However, to ensure ITs cytotoxicity, it is also important to choose the most potent toxin available, allowing the use of a lower number of internalized molecules
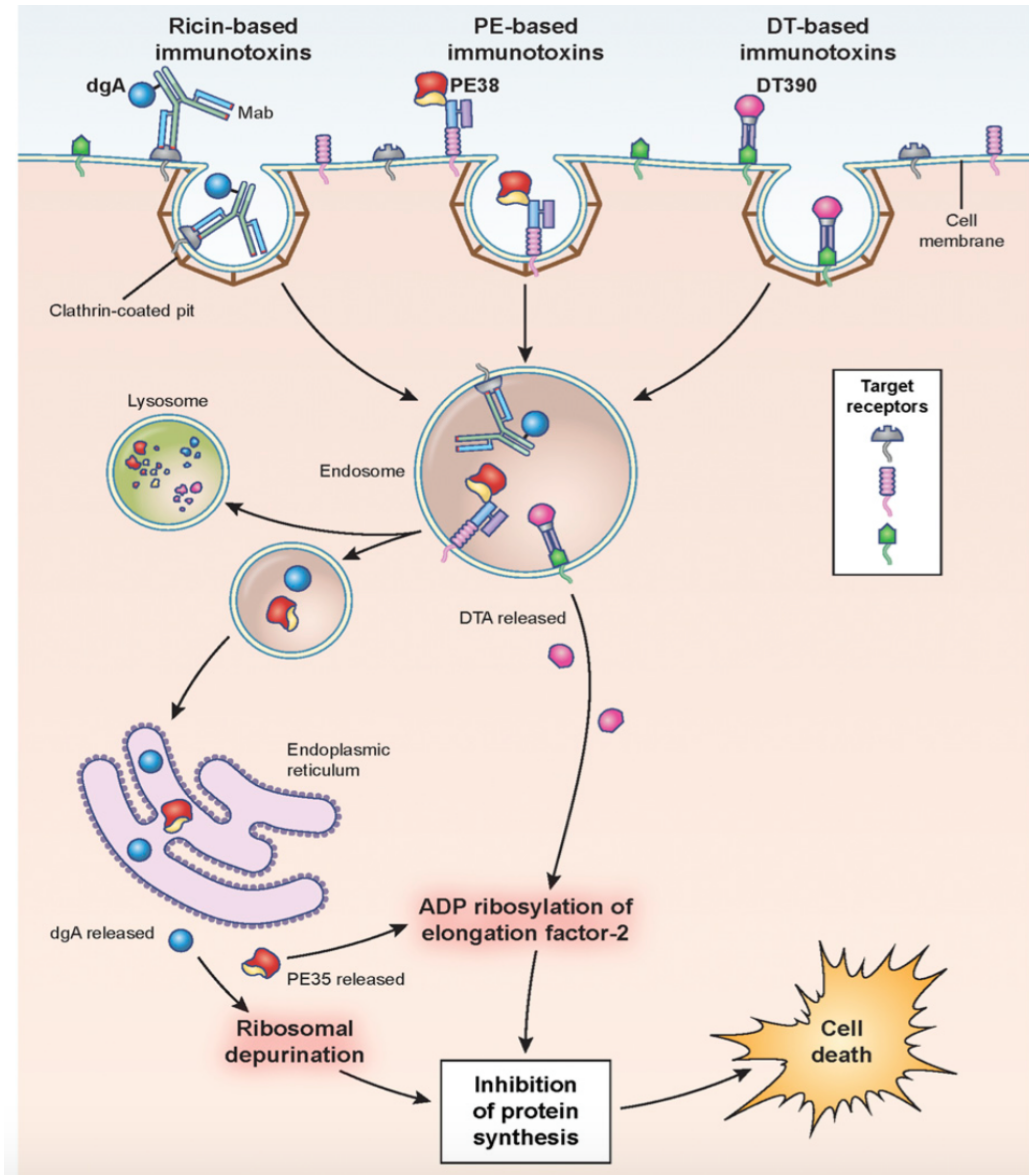
Figure 4 Pathways of binding, internalization, and processing by ITs leading to the killing of target cells. Shown are ricin-, PE- and DT-based ITs. ITs bind the target antigen, are internalized via clathrin-coated pits, and are processed within endosomal compartments. Ricin and PE toxin derivatives must traffic through the endoplasmic reticulum to the cytosol where they enzymatically inactivate protein synthesis. PE ADP-ribosylates eEF-2, while Ricin depurinates ribosomal RNA. DT-based toxins are internalized to endosomes where the A chain of the toxin translocates directly to the cytosol and ADP-ribosylates eEF-2. Cell death follows inhibition of protein synthesis. dgA: deglycosylated Ricin A chain. Adapted from Wayne, A. *et al.*, (2014).

1.4 Breast Cancer

Breast cancer is the most common cancer diagnosed among women in United States of America alone [40]. According to the American Cancer Society, in 2018 breast cancer was estimated to kill approximately 40,920 women[41]. Gene expression profiling of breast cancer tissues is still a costly and complex process; however, it is the best way not only to identify biological biomarkers but to help in the development of new pharmaceuticals against these biomarkers. There are four main molecular subtypes, depending on the expression of HER2 and on hormone receptors (HR): Luminal A ($HR^+/HER2^-$); Luminal B ($HR^+/HER2^+$); HER2-enriched ($HR^-/HER2^+$) and triple negative ($HR^-/HER2^-$) [42].

1.4.1 HER2$^+$ Breast Cancer

Figure 5 Transduction by the HER family. There are four members of the HER family: HER1, HER2, HER3, and HER4. There are receptor-specific ligands for HER1, HER3, and HER4. An intracellular tyrosine kinase domain exists for HER1, HER2, and HER4. Phosphorylation of the tyrosine kinase domain by means of homodimerization or heterodimerization induces both cell proliferation and survival signalling. HER2 is the preferred dimerization partner for the other HER family members. The phosphorylated tyrosine residues on the intracellular domain of HER2 activate the lipid kinase phosphoinositide 3-kinase (PI3-K), which phosphorylates a phosphatidylinositol that in turn phosphorylates the enzyme Ak transforming factor (Akt), driving cell survival. In parallel, a guanine nucleotide exchange factor, the mammalian homologue of the son of seven-less (SOS), activates the rat sarcoma (RAS) enzyme that activates the receptor activation factor (RAF) and then the mitogen extracellular signal kinase (MEK) and the mitogen-activated protein kinase (MAPK), the phosphorylated MAPK, drives cellular proliferation. One of many other downstream effects is the production of vascular endothelial growth factor (VEGF) supporting angiogenesis. Adapted from Hudis, C. A., (2007).

Approximately 20 % of breast cancer patients have shown to have an overexpression of the c-*erb*B-2 oncogene which encodes the HER2 protein; these patients also have poor prognosis due to a shorter survival rate and time to relapse [43]. The HER family is composed by four homologous receptors involved in cell growth, differentiation and survival. These four receptors exist as monomers in the cell membrane and are activated by binding to a wide range of growth factor ligands enabling the formation of homo or heterodimers leading to signal transduction by activation of their tyrosine kinase domains, ultimately inducing gene activation (Figure 5) [44].

The HER2 receptor is the exception in the family. Since there are no known ligands, this receptor is able to dimerize with all receptors of the family independently of ligand binding. Therefore, overexpression of HER2 in cancer cells enhances signal transduction and potentiates cell growth and survival of these malignant cells leading to overgrowth tumor masses. For these reasons, HER2 has been studied as a marker for target therapy.

1.4.2 Trastuzumab – Targeted therapy against HER^{2+} Cancer

The biopharmaceutical Trastuzumab (Herceptin®), a humanized mAb (Immunoglobulin G1 - IgG1) that targets the extracellular domain of the HER2 receptor, was the first major breakthrough in HER2$^+$ breast cancer targeted therapies. It is currently used on the first-line of treatment conjugated with chemotherapy in patients with this type of cancer, leading to the increase of response rate, progression-free survival and overall survival of these patients [45] when compared with other treatments.

There are four major known mechanisms by which Trastuzumab can reduce the HER2 signalling pathway, therefore diminishing cancer cell proliferation: prevention of HER2 receptor cleavage, and thus formation of truncated p95 HER2 (Figure 6A); prevention of HER2 receptor dimerization with other family receptors (Figure 6B); activation of an antibody-dependent cell-mediated cytotoxicity (ADCC) mechanism (Figure 6C); and increase of HER2 degradation by enhancing internalization (Figure 6D) [46].

By inhibiting the binding of HER2 receptor to the other members of the Epidermal Growth Factor Receptor (EGFR) family and by blocking the metalloprotease cleavage site in the HER2 extracellular domain [47], Trastuzumab can hamper the mitogen-activated protein kinase (MAPK) and phosphoinositide 3-kinase (PI3K) signalling pathways increasing cell cycle arrest and suppression of cell growth and proliferation [48]. As a monoclonal humanized IgG1 with a Fragment crystallizable (Fc) region, Trastuzumab is able to recruit immune cells such as Natural Killer cells, which will lead to the death of cancer cells by a CD16 mediated ADCC mechanism [49].

HER2 degradation by Trastuzumab binding and internalization of the receptor is the most controversial mechanism of Trastuzumab action. Unlike the receptor tyrosine-protein kinase erbB-1 (HER1) receptor, known to be endocytosed and degraded upon ligand-induced homodimerization, HER2 has no known ligands and its dimerization and endocytosis with other receptors generates an unstable state of dimerization and so it is often recycled to the cell membrane [50].

Though it is known that the binding of Trastuzumab to the HER2 receptor may recruit the c-Cbl protein, a well-known ubiquitin ligase that can ubiquitinate HER2 and label it for lysosomal degradation [51], the actual binding affinity of the c-Cbl protein to HER2 when compared to HER1 it is still very low. Therefore, it is possible that although Trastuzumab-HER2 binding leads to endocytosis, it may not lead to its degradation. New methods to enhance HER2 degradation have been studied, one very promising method is the clustering of receptors in cell surface [52]. Moody *et al.* were able to cluster the HER2 receptor and induce lysosomal degradation by using biotinylated Trastuzumab and streptavidin.
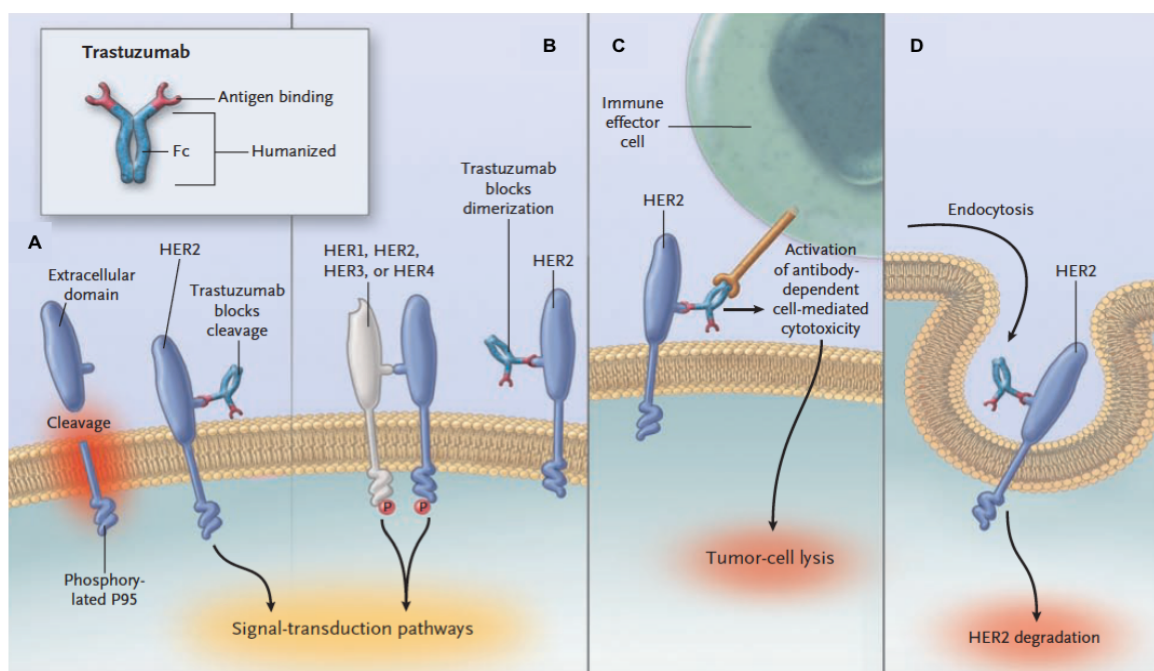
Figure 6 The most well-documented potential Trastuzumab mechanisms of action are shown in A through D. **A)** Binding of Trastuzumab to a juxtamembrane domain of HER2 reduces shedding of the extracellular domain, thereby reducing p95. **B)** Trastuzumab may reduce HER2 signalling by physically inhibiting either homodimerization or heterodimerization. **C)** Trastuzumab may recruit Fc-competent immune effector cells and the other components of antibody-dependent cell-mediated cytotoxicity, leading to tumor-cell death. **D)** Additional mechanisms such as receptor down-regulation through endocytosis have been postulated. Adapted from Hudis, C. A., (2007).

1.5 Objective

The aim of this project is to construct a new model of IT, a proimmunotoxin (PIT), for usage in HER2$^+$ breast cancer therapy. The A chain of Ricin toxin will function as the killing moiety of the PIT that will be delivered by a chimeric Trastuzumab. This antibody will be linked to an anti-Ricin A VHH homodimer that will neutralize Ricin A until it reaches the target cell. Upon internalization of the PIT by the cancer cell, the low pH present in the endosomes will allow the release of Ricin A as an active substance, arresting protein synthesis and inducing apoptosis in breast cancer cells.

With this project, we hope to overcome side-effects produced by the non-specific toxicity of the active toxin during blood circulation, an existing problem of ITs in breast cancer treatment. By using this technology even Trastuzumab resistant tumors will be accessible to treatment. In cases which resistance to Trastuzumab appears due to the expression of other tyrosine kinase receptors in the cellular membrane, Trastuzumab will still be able to deliver the toxin to kill the cancer cell by HER2 binding. This new and state-of-the-art approach can later be used as a model for other antibody treatments that generate patient resistance to the treatment.
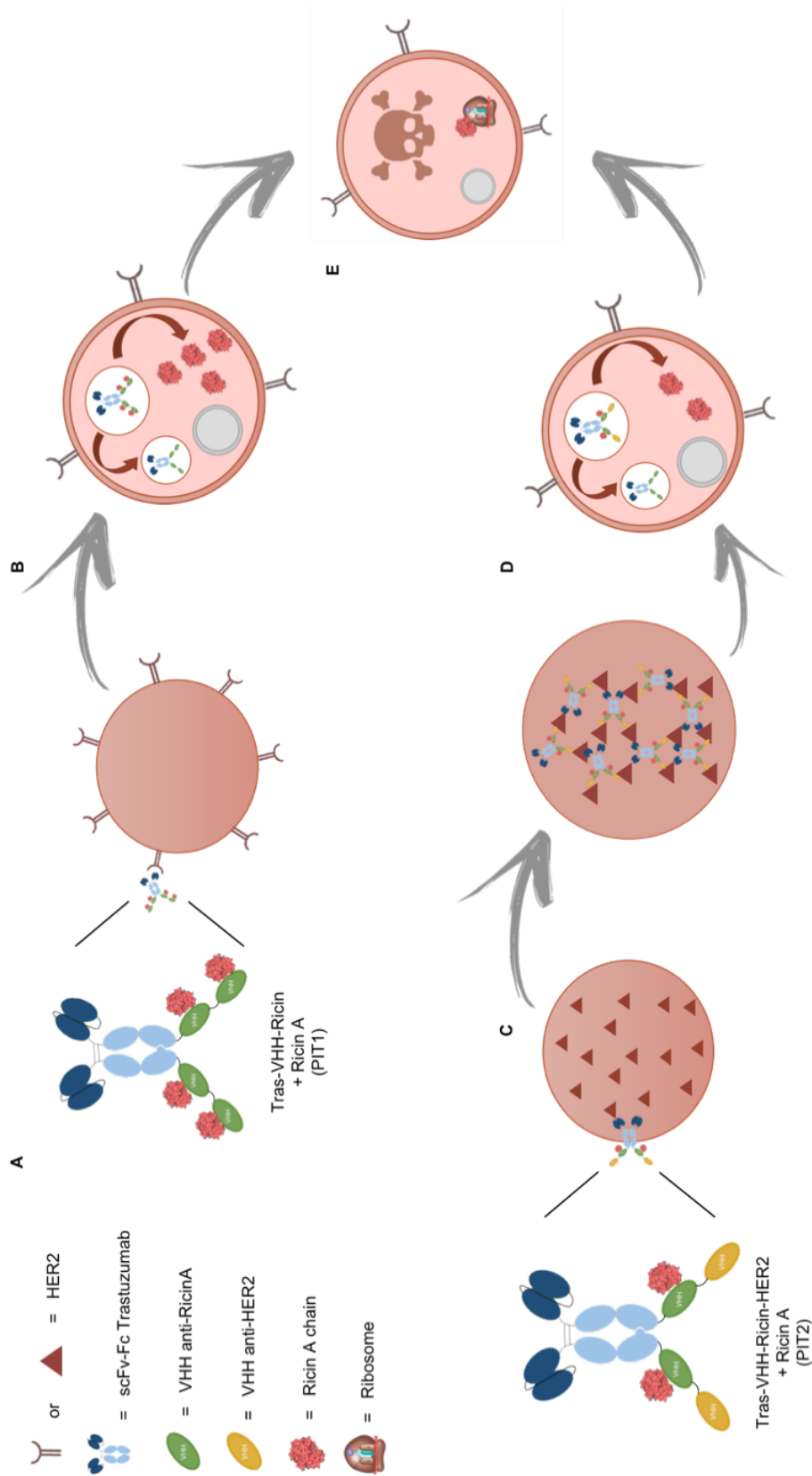
Figure 7 PIT mechanisms of action. **A)** PIT1 is composed of a scFv-Fc Trastuzumab coupled with two VHH homodimers capable of binding to Ricin A chain. This PIT will bind to a HER2 protein. **B)** PIT1 binding will lead to its internalization, in the endosomes binding of VHH to Ricin A chain is disrupted and RicinA is released to the cytosol. **C)** PIT2 is composed of a scFv-Fc Trastuzumab coupled with two VHH heterodimers capable of binding to Ricin A chain and to HER2. This PIT will bind to a HER2 protein by two different epitopes, clustering the HER2 at the cell membrane enhancing its internalization. **D)** PIT2 binding and clustering will lead to its internalization, in the endosomes binding of VHH to Ricin A is disrupted and Ricin A is released to the cytosol. **E)** In the cytosol Ricin A will bind to the ribosome halting protein synthesis resulting in cell death.

2. Materials and Methods

2.1 Bacterial Strains and Media

Escherichia coli XL-1 Blue (Stratagene, San Diego, California, EUA) and JM109 (Promega, Madison, Wisconsin, EUA) were used for plasmid propagation (bacterial genotypes shown in Annexes 7.1). These bacterial strains were grown in LB medium (10 g tryptone; 5 g yeast extract in 1L dH2O) supplemented with ampicillin to a final concentration of 0.1 mg/mL according to the plasmid selectable marker. Incubations were carried out at 37 ºC, 220 rpm. Electrocompetent bacteria were transformed with the plasmid of interest following the manufacturer's protocol. For plasmid extraction, NucleoBond® Xtra Midi (Macherey-Nagel, Düren, Germany) columns were used.

2.2 Cell Lines and Culture Conditions

Four different cell lines were used during this work: Human Embryonic Kidney 293T (HEK293T) cells (ATCC, Manassas, Virginia, EUA), FreeStyle™ 293-F (ThermoFisher, Waltham, Massachusetts, EUA), SK-BR-3 [SKBR3] (ATCC) (derived from Human Mammary Breast Adenocarcinoma) and HeLa P4 (NIH, Bethesda, Maryland, EUA) (derived from Human Cervix Adenocarcinoma, expressing CD4 and CCR5).

Adherent cell lines (HEK293T, SKBR3 and HeLa P4) were cultured at 37ºC with 8% of CO_2 in Dublbecco's Modified Eagle's Medium (DMEM) (Lonza, Basel, Switzerland) supplemented with 10% (v/v) FBS (Biowest, Nuaillé, France), 2 mM L-Glutamine (Lonza) and PSA (100 U Penicillin, 100 µg Streptomycin, 0.25 µg Amphotericin B) (Lonza) [DMEM+/+].

FreeStyle™ 293-F cell line was cultured at 37 ºC with 8% of CO_2 at a constant rotation of 125 rpm in FreeStyle™ 293 Expression Medium (ThermoFisher). FreeStyle™ 293-F cell line was used for antibody production.

2.3 Cell Transfection

HEK293T and FreeStyle™ 293-F cells were transfected using Polyethylenimine (PEI) (Polysciences, Warrington, Pennsylvania).

HEK293T were seeded at a density of $3x10^5$ cells per well in 6-well plates (Orange Scientific, Braine-l'Alleud, Belgium). After 24 h, cell medium was changed to a total volume of 3 mL for non-transfected wells and 2.7 mL for transfected wells. PEI (1 mg/mL) was diluted in a total volume of 150 µL of DMEM, 4.5 µg or 9 µg, and respectively 1.5 µg or 3 µg of DNA were diluted in a total volume of 150 µL of DMEM, for a ratio of 1:3 (DNA:PEI). Diluted PEI

was added to diluted DNA, the mixture incubated for 30 min at room temperature [r.t.] and then added to the cells. After 72 h of incubation, cells and cell medium were harvested for analyses of protein expression and secreted proteins by Western Blot.

FreeStyle™ 293-F were seeded at a concentration of ~ $5x10^5$ cells/mL (total volume of 100 mL ~ $5x10^7$ cells). After 24 h, cells were counted using trypan blue staining to ensure cell density of $1x10^6$ cells/mL and cell viability higher than 95%. DNA (100 µg) was diluted in 5 mL of DMEM and PEI (300 µg) was also diluted in 5 mL of DMEM. Diluted PEI was added to diluted DNA in a ratio of 3:1, the mixture incubated for 15 min at r.t. and then added to the cells for transfection. Seven days later, cell medium was harvested for antibody purification by Protein A affinity chromatography.

2.4   Affinity Chromatography

Transfected 293-F cell medium (≈100 mL) was recovered 7 days after transfection and filtrated using a 0.45 µm filter (Sarstedt, Nümbrecht, Germany). The filtrate was then concentrated to a final volume of 2.5 mL using an Amicon® Ultra 50K device (Merck Millipore, Burlington, Massachusetts, EUA) and diluted 1:2 with Phosphate Buffered Saline (PBS) (155.17 mM NaCl, 2.97 mM $Na_2HPO_4 \times 7H_2O$, 1.06 mM KH_2PO_4, pH 7,4).

For the purification of secreted antibodies, a 1 mL HiTrap™ Protein A Shepharose Column (GE Healthcare, Chicago, Illinois, EUA) was used, coupled to the Bio-Rad Biologic Workstation (BioRad, Hercules, California, USA) using the Biologic v1.30 (BioRad) software. Prior to sample injection the column was rinsed with 10 mL of PBS, sample injection was made through a static loop with a flow rate of 0.5 mL/min. Following sample injection, the column was washed with 10 mL of PBS at a flow rate of 1 mL/min and antibody elution performed with 8 mL of 0.5 M Acetic Acid at a flow rate of 1 mL/min. In the end, the column was washed with 20 mL of PBS, 5 mL of ultra-pure H_2O followed by 5 mL of 20% (v/v) ethanol and stored at 4 ºC.

Elution fractions were collected in fraction collector Frac 2110 (BioRad) to a final volume of 0.5 mL and then added 0.65 mL of 1 M Tris-HCL (pH 8). Fractions containing antibodies were identified by measuring absorbance at 280_{nm} using an Ultraviolet (UV) photometer (ThermoFisher) (NanoDrop® 1000 Spectrophotometer) and analysed by SDS-PAGE and Western Blot.

2.5   SDS-PAGE

Recovered transfected cells were lysed with Radio-Immunoprecipitation assay (RIPA) buffer (NaCl 150 mM; 1% (v/v) Nonidet-P40; 0.5% (w/v) Sodium deoxycholate; 0.1% (w/v) SDS; 50 mM Tris, pH 8) supplemented with cOmplete™ Protease Inhibitor Cocktail (Roche, Basel, Switzerland). Cells were centrifuge for 30 min at 16000 xg, after incubation with RIPA buffer for 30 min, cellular extract was recovered from supernatant.

Samples recovered from HEK293T transfection, cellular extract and cell medium were prepared with to have 50 ng of protein. Total protein concentration was determined using Bio-Rad Protein Assay Dye Reagent Concentrate (BioRad). Calibration curve was obtained by analyses of a series of standard solutions of bovine serum albumin (BSA) (GBiosciences, St. Louis, Missouri, USA) ranging between 200 and 3.125 mg/mL. BSA standards were prepared in duplicate and subjected to the same procedure as samples. Linear regression analysis of the data gave correlation coefficients between 0.9694 and 0.9995.

Samples of antibody purification were all prepare with the same volume of 22 µL. Prior to sample loading, loading buffer (50 mM Tris-HCl pH 6.8; 2% (w/v) SDS; 10% (v/v) Glycerol; 0.1% (w/v) Bromophenol Blue; 100mM Dithiothreitol) was added to samples and they were then heated for 10 min at 95 ºC. Samples were loaded in a 12% (w/v) polyacrylamide resolving gel using the Mini-PROTEAN® Tetra Cell (BioRad). In parallel molecular weight marker PageRuler (ThermoFisher) was loaded in the gel. Electrophoresis proceeded at constant 180 V during resolving run. Afterwards, gels were stained with BlueSafe (Nzytech, Lisbon, Portugal) for protein visualization.

2.6   Western Blot

For Western Blot analyses, proteins in SDS-PAGE gels (not stained) were transferred to a Nitrocellulose 0.45 µm membrane (GE Healthcare) for 90 min at constant current of 250 mA at 4 ºC in a Mini Trans-Blot® Cell (BioRad). Membranes were then blocked with 5% (w/v) of non-fat dry milk (Nestlé, Vevey, Switzerland) in 0,1% (w/v) Tris Buffered Saline-Tween (TBS-T) (8.77 g NaCl, 10 mL 1M Tris-Cl pH 7.5, 1 mL Tween-20 in 1 L ddH$_2$O) for 1h at r.t.. Membranes were washed four times for 15 min with 0.1% TBS-T prior to incubation with antibody. For cellular extract samples the primary antibody used was a mouse anti-β-Actin monoclonal antibody (Sigma, Darmstadt, Germany), prepared in 1% (w/v) of non-fat dry milk in 0.1% TBS-T (1:15000) for 1h at r.t.. Membranes were washed again in the same conditions and then incubated with secondary antibodies, both prepared in 1% of non-fat dry milk in 0.1% TBS-T, a goat anti-Mouse IgG HRP conjugated (BioRad) (1:3000) and a goat

anti-Human IgG HRP conjugated (ThermoFisher) (1:5000), for 1h at r.t.. For cell supernatant samples and samples from fractions collected after purification the only antibody used was the goat anti-Human IgG HRP conjugated (ThermoFisher) (1:5000), incubated for 1h at r.t..

Before membrane development, membranes were rewashed in the same conditions. Membrane development was made using SuperSignal™ West Pico PLUS Chemiluminescent Substrate (ThermoFisher) and images acquired using Molecular Imager® ChemiDoc™ XRS System (BioRad).

2.7   Flow Cytometry

Cells were collected from flasks with cell dissociation buffer (0.6 nM EDTA) and centrifuged at 300 xg for 5 min, and then resuspended in 3% (w/v) BSA (Sigma) in PBS to a final concentration of 1 x 10^6 cells/mL. Cell suspension was aliquoted in 100 µL (1 x 10^5 cells) and incubated with primary antibody (Trastuzumab, Tras-VHH-R and Tras-VHH-R-H) to a final concentration of 0.08, 0.8, 8 and 80 nM for 30 min. Cells were then washed twice with 3% BSA/PBS and subsequently incubated with the secondary antibody goat anti-Human IgG FITC-conjugated (ThermoFisher) to a final dilution of 1:400. Cells were washed at least two times with 3% BSA/PBS and 10 µL of propidium iodide (10 µg/mL, Sigma) was added to stain dead cells. Assessment of antibody binding were performed using Guava easyCyte™ (Merck Millipore). Incubation periods were made at 4 ºC. Flow cytometry data was analysed with FlowJo software (TreeStar).

2.8   Enzyme-Linked Immunosorbent Assay (ELISA)

Corning® 96-well High Bind Microplates were coated overnight at 4ºC with 1 ng/ µL of Ricin A-Chain (Sigma) diluted in PBS, blocked for 1h with 2% BSA/PBS at 37 ºC. The microplates were incubated with serial dilutions ranging from 1:10 to 1:300000 of primary antibody Trastuzumab, Tras-VHH-R and Tras-VHH-R-H for 1h at 37 ºC. Next, plates were washed 3 times with 0.1% PBS-Tween (PBS-T) and incubated with secondary antibody goat anti-Human IgG HRP-conjugated (dilution 1:20000, ThermoFisher) for 30 min at 37 ºC. Both antibodies were prepared in 1% BSA in 0.1% PBS-T. Finally, plates were washed thrice with 0.1% PBS-T and developed with 3,3',5,5'-Tetramethylbenzidine (TMB) (Merck Millipore), according to the manufacture's protocol, absorbance was measured at 450 nm in a Microplate Reader (BioRad, Model 680 Microplate Reader).

2.9   Methylthiazolyldiphenyl-tetrazolium bromide (MTT) Assay

For MTT assays, HeLa P4 and SKBR3 cell lines were used. Cells were seeded at a density of ~ 3 x 10^4 cells/mL in a 96 well plate (Sarstedt). After 24h, cell medium was exchanged, and cells incubated with different concentrations of antibody (0.08, 0.8, 8 and 80 nM; Tras-VHH-R and Tras-VHH-R-H), (0.1, 0.2 and 2 nM) Ricin A-Chain and PIT (prepared in cell medium). Cells were incubated for 48h and 72h at 37 ºC with 5% CO_2. After incubation time, cells were washed with PBS and subsequently incubated with 100 µL of PBS and 10 µL of MTT (Sigma) (5 mg/mL) for 45 min at 37 ºC with 5% CO_2. Finally, incubation medium was discarded and formazan crystals were dissolved in 100 µL of Dimethyl sulfoxide (DMSO) (Sigma), absorbance was measured at 490_{nm} in a Microplate Reader (BioRad, Model 680 Microplate Reader). Percentage of cell viability was then determined through the absorbance at 490_{nm} non-treated cells subjected to MTT assay.

3. Results

For the construction of Tras-VHH-R antibody which composes PIT1, the sequence encoding the homodimer anti-Ricin A VHH (RTA-D10) [53,54] was subcloned into the mammalian expression vector pCEP4-Trastuzumab using HindIII and XhoI restriction enzyme [pCEP4-VHH-R]. For Tras-VHH-R-H antibody which composes PIT2, the anti-Ricin A (RTA-D10) and anti-HER2 [55] VHH sequences were also subcloned into the pCEP4-Trastuzumab vector using HindIII and XhoI [pCEP4-VHH-R-H]. The vector pCEP4 was previously cloned with a fragment encoding Trastuzumab in an scFv-Fc format, which was kindly provided by Dr. Christoph Rader [56]. The pCEP4-Tratuzumab vector encodes a peptide leader that will allow the secretion of antibodies encoded in this vector. (Plasmid maps are shown in Annexes 7.2)

3.1 Small scale production of antibodies

This work initiated with the objective to transfect HEK293T cells with plasmids containing the desired antibodies for PIT construction (pCEP4-Trastuzumab, pCEP4-VHH-R and pCEP4-VHH-R-H), to confirm protein expression and secretion by these cells. For this, HEK293T cells were transfected with different DNA quantities (1.5 µg or 3 µg), always with ratio of 3:1 of PEI:DNA. After 72h of transfection either cells and cell medium were recovered to assess antibody expression in the cellular extract and antibody secretion in cell medium. At the recovery point it was possible to observe a colour change in the medium between transfected wells and also between transfected and non-transfected wells, suggesting a difference in cell growth (Figure 8).

pCEP4   pCEP4 VHH-R   pCEP4 VHH-R-H
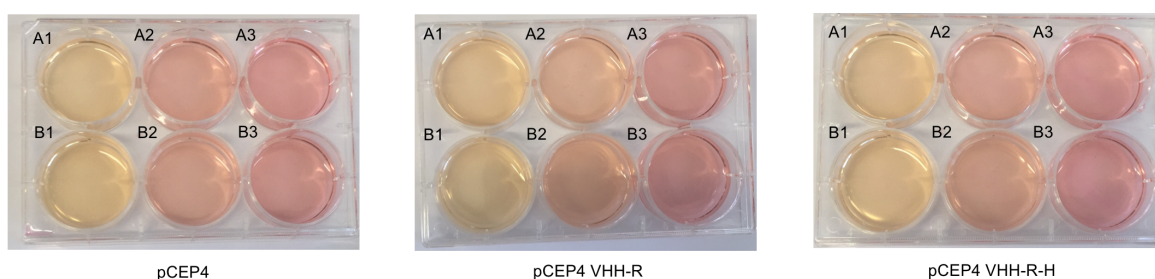
Figure 8 HEK293T were seeded at a density of $3x10^5$ cells per well in 6-well plates 24h prior to transfection. A1 and B2 non-transfected cells. A2 and B2 cells transfected with 1.5 μg DNA, 1:3 Ratio DNA:PEI. A3 and B3 cells transfected with 3 μg DNA, 1:3 Ratio DNA:PEI. Photograph was taken 72h after transfection, prior to cell and cell medium were harvested.

The presence of phenol red in cell medium allows a correlation between cell medium colour and cell growth through the decrease of pH with increase of cell number and metabolic activity.

Correlation between the colour medium and cell number was confirmed by observation of the wells in an optical microscope, cell number decreased from non-transfected wells (A1 and B1) to wells transfected with 1.5 µg (A2 and B2) of DNA, and subsequently to wells transfected with 3 µg of DNA.

pCEP4

pCEP4 VHH-R
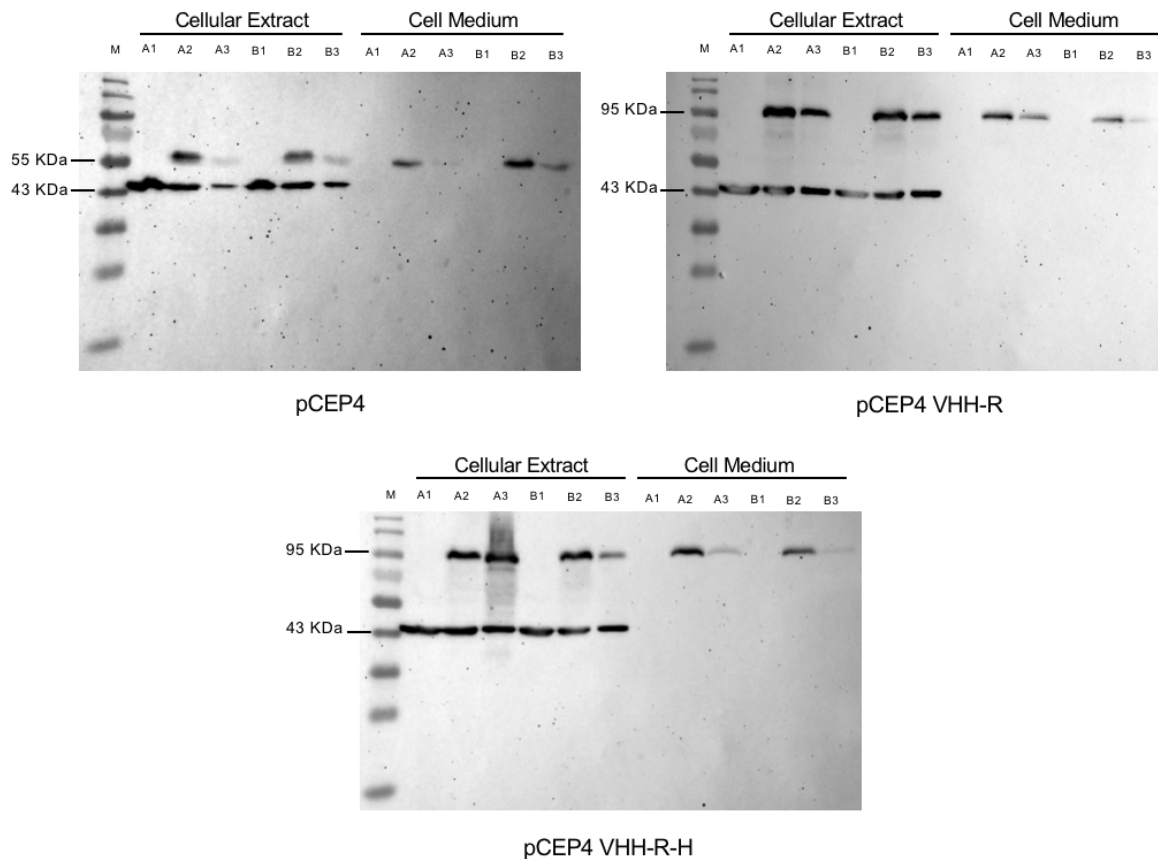
pCEP4 VHH-R-H

Figure 9 Assessment of HEK293T cells with pCEP4-Trastuzumab, pCEP4 VHH-R and pCEP4 VHH-R-H by Western-Blot. A1 and B1 non-transfected cells. A2 and B2 cells transfected with 1.5 μg DNA, 1:3 Ratio DNA:PEI. A3 and B3 cells transfected with 3 μg DNA, 1:3 Ratio DNA:PEI. M) Molecular weight marker.

Western-Blot revealed in all lanes of the cellular extract a band at ~43 KDa, consistent with the expression of β-Actin, loading control for this experiment. It is also possible to observe bands at ~55 KDa on lanes A2, A3, B2 and B3 for both cellular extract and cell medium of cells transfected with pCEP4-Trastuzumab corresponding to the expression and secretion of Trastuzumab antibody. Bands at ~95 KDa on lanes A2, A3, B2 and B3 for both cellular extract and cell medium of cells transfected with pCEP4-VHH-R and pCEP4-VHH-R-H, correspond to the expression and secretion of antibody Tras-VHH-R and Tras-VHH-R-H, respectively.

Bands corresponding to the expression of Trastuzumab, Tras-VHH-R and Tras-VHH-R-H in lanes A2 and B2, which correspond to cells transfected with 1.5 µg of DNA, show a higher intensity then those corresponding to cells transfected with 3 µg of DNA (A3 and B3), in both cellular extract and cell medium. The intensity of bands corresponding to the desired antibodies is also in correlation with colour change observed in cell medium of cells transfected with 1.5 µg and 3 µg (Figure 9).

With these results, it is possible to confirm the expression and secretion to the medium of the desired antibodies, allowing therefore their large scale production and purification.

3.2   Large scale production and purification of antibodies

FreeStyle™ 293-F cell line was chosen for the large scale production of the desired antibodies due to its capacity of transfection in high volumes and cell density. According to the previous results, cells were transfected with low quantity of DNA to ensure preservation of cell viability with transfection and antibody production (100 µg of DNA in 5×10^7 cells).

Cells were transfected with the different plasmids pCEP4-Trastuzumab, pCEP4-VHH-R and pCEP4-VHH-R-H. After the period of incubation, cell medium was recovered and treated according protocol for purification with Protein A chromatography.

This purification technique is based on the affinity between the Staphylococcal protein A, a cell wall protein present in the bacterium *Staphylococcus aureus*, which is cross-linked to a column matrix (Sepharose) and the Fc region of various IgG antibodies. During sample load, IgG antibodies are retained in the column [57], while other proteins are eluted in the flow through. A pH buffer change to a more acidic pH will disrupt the binding of the antibodies to protein A. The recovered antibody fractions need the addition of a Tris based buffer, with a basic pH to neutralize the elution buffer pH.

The backbone of the antibodies Tras-VHH-R and Tras-VHH-R-H is Trastuzumab in a scFv-Fc format, the Fc portion of these three antibodies allows their purification by protein A affinity chromatography.

The chromatograms in Figures 10, 11 and 12, correspond respectively to the purification of Trastuzumab, Tras-VHH-R and Tras-VHH-R-H. From these chromatograms, it is possible to observe an increase in absorbance in the initial fractions 1 and 2, which correspond to the flow-through of column injection (unbound protein). In each chromatogram, a peak is observed at the time of elution buffer (Buffer B) injection, concurring with the decrease in conductivity, due to the lack of salts in this buffer. The peak occurs in fractions 8 to 12 for Trastuzumab, 14 to 21 for Tras-VHH-R and 23 to 26 for Tras-VHH-R-H. These fractions most likely correspond to antibody containing fractions.
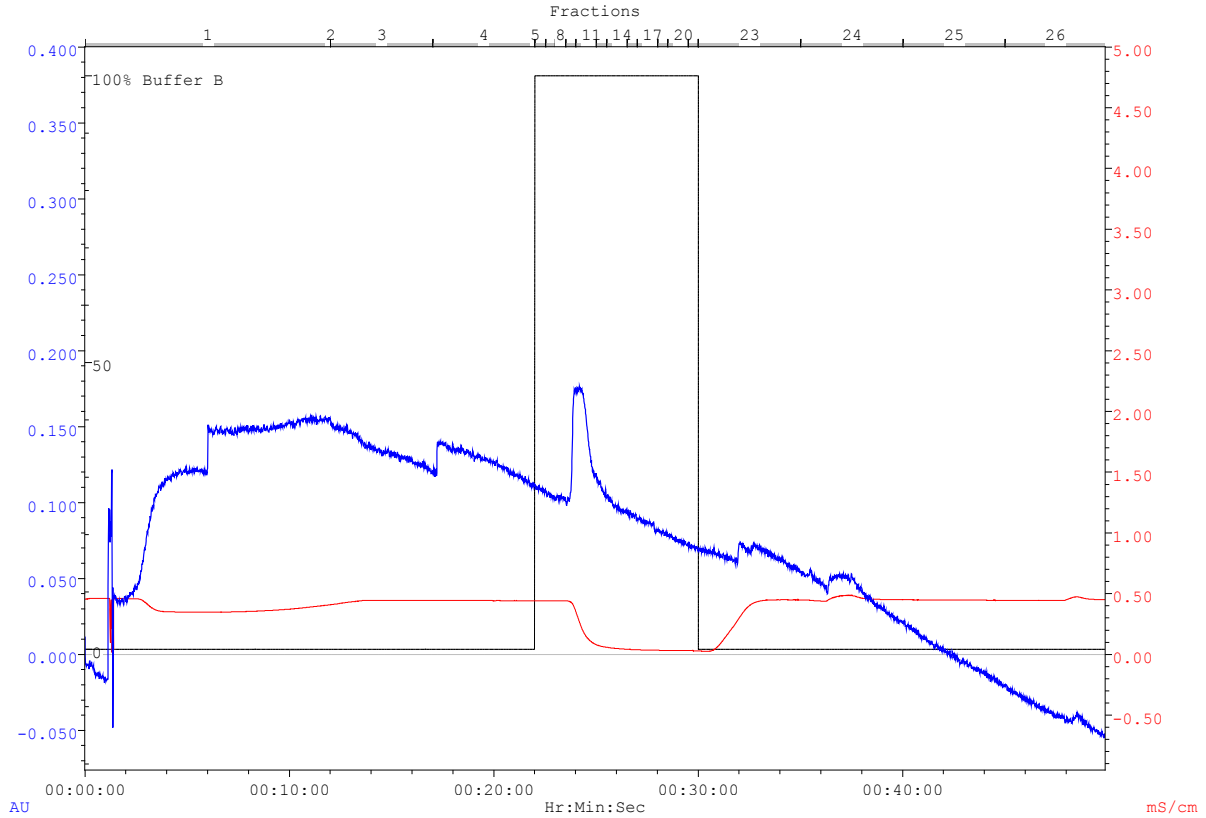
Figure 10 Chromatogram obtained after the Trastuzumab purification using the Bio-Rad Biologic Workstation (BioRad) coupled with a HiTrap™ Protein A HP Column (GE Healthcare Life Sciences), acquired with Biologic v1.30 software (BioRad). In the left y axis is represented the absorbance at 280_{nm} (AU), in the right y axis is represented the conductivity (mS/cm) and in the x axis is represented time (hours:minutes:seconds). The black line corresponds to the percentage of elution buffer (0.5 M Acetic Acid, Buffer B) during purification. At the top of the chromatogram is represented the different fractions collected over time. The chromatogram was obtained as described in Materials and Methods.
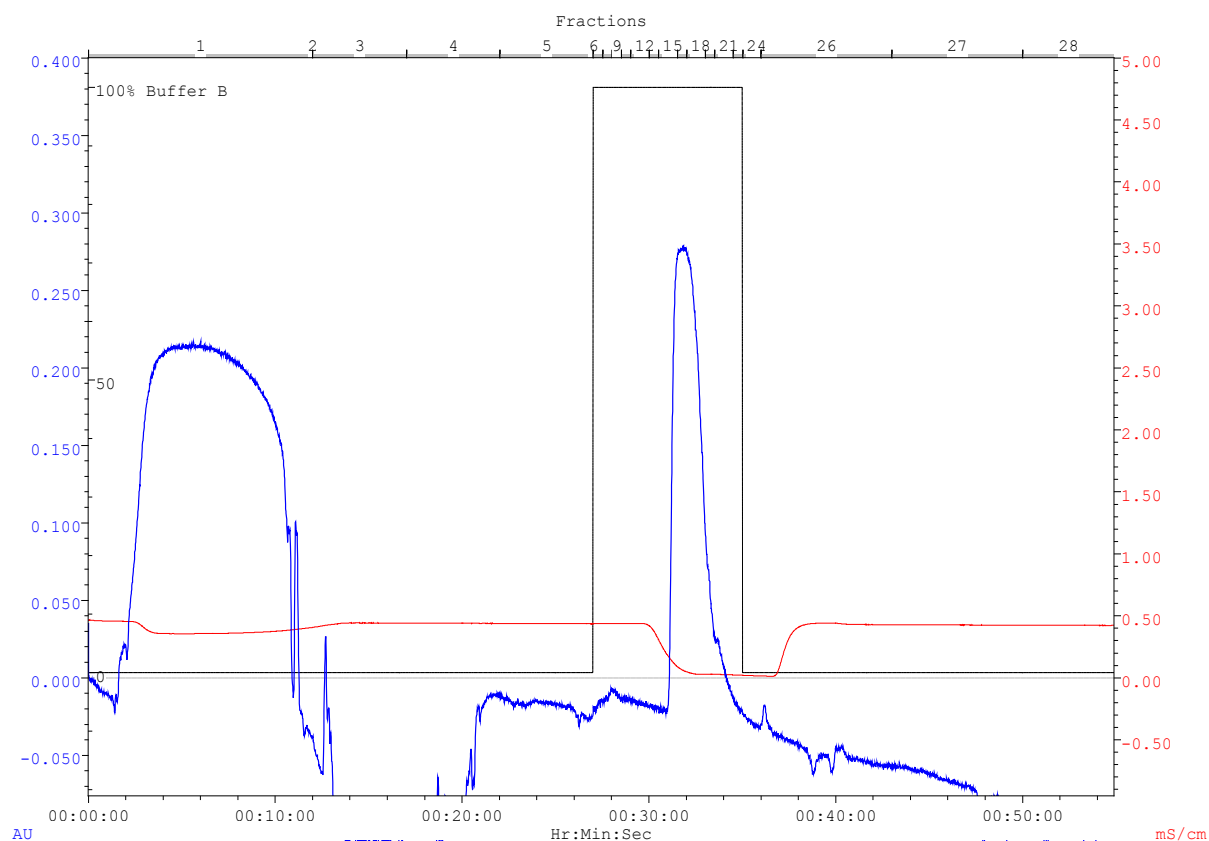
Figure 11 Chromatogram obtained after the Tras-VHH-R purification using the Bio-Rad Biologic Workstation (BioRad) coupled with a HiTrap™ Protein A HP Column (GE Healthcare Life Sciences), acquired with Biologic v1.30 software (BioRad). In the left y axis is represented the absorbance at 280_{nm} (AU), in the right y axis is represented the conductivity (mS/cm) and in the x axis is represented time (hours:minutes:seconds). The black line corresponds to the percentage of elution buffer (0.5 M Acetic Acid, Buffer B) during purification. At the top of the chromatogram is represented the different fractions collected over time. The chromatogram was obtained as described in Materials and Methods.
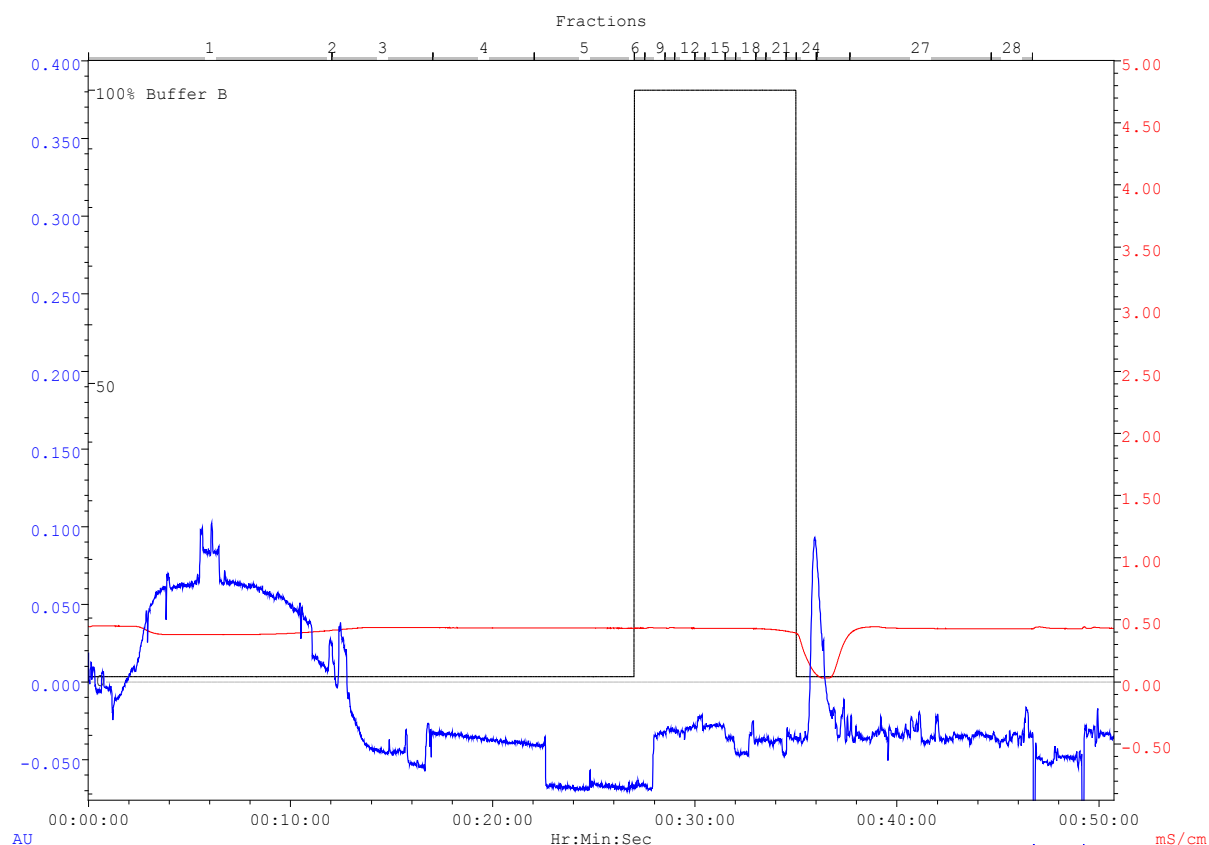
Figure 12 Chromatogram obtained after the Tras-VHH-R-H purification using the Bio-Rad Biologic Workstation (BioRad) coupled with a HiTrap™ Protein A HP Column (GE Healthcare Life Sciences), acquired with Biologic v1.30 software (BioRad). In the left y axis is represented the absorbance 280_{nm} (AU), in the right y axis is represented the conductivity (mS/cm) and in the x axis is represented time (hours:minutes:seconds). The black line corresponds to the percentage of elution buffer (0.5 M Acetic Acid, Buffer B) during purification. At the top of the chromatogram is represented the different fractions collected over time. The chromatogram was obtained as described in Materials and Methods.

Although the three chromatograms presented above show a clear peak at the elution step, which indicates antibody elution, to better assess protein purification and fractions containing antibody, an SDS-PAGE and Western-Blot were performed. Fractions used in SDS-PAGE and Western-Blot analyses were chosen according to the absorbance at 280_{nm} (Table 2, 3 and 4 with absorbance's are shown in Annexes 7.3).
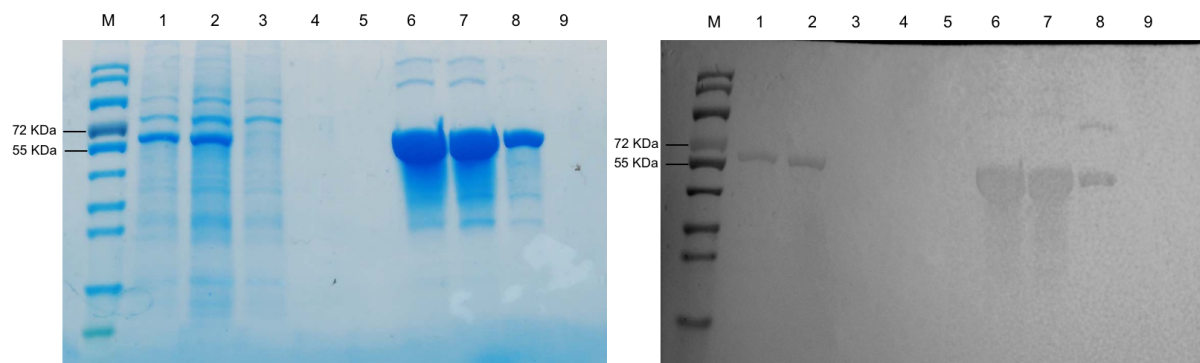
Figure 13 Assessment of Trastuzumab purification using Protein A affinity chromatography by SDS-PAGE (left) and Western-Blot (right). 1) Medium of cells secreting Trastuzumab. 2) Medium of cells secreting Trastuzumab concentrated by Amicon. 3) Flow-through of Trastuzumab medium – Fraction 1. 4) Column wash after Trastuzumab loading – Fraction 2. 5) Column wash after Trastuzumab loading – Fraction 3. 6) Fraction 9 of Trastuzumab elution. 7) Fraction 10 of Trastuzumab elution. 8) Fraction 11 of Trastuzumab elution. 9) Column wash after Trastuzumab elution – Fraction 22. M) Molecular weight marker.

By observation of bands presented at ~55 KDa on lanes 1, 2, 6, 7 and 8 in the SDS-PAGE (Figure 13), it is possible to confirm the production of the antibody Trastuzumab by the cells and its successful purification by Protein A chromatography. Through Western-Blot technique, it is possible to confirm that the bands presented at ~55 KDa in SDS-PAGE correspond to the antibody Trastuzumab, using an anti-Human IgG HRP conjugated for detection of the Fc region in Trastuzumab.
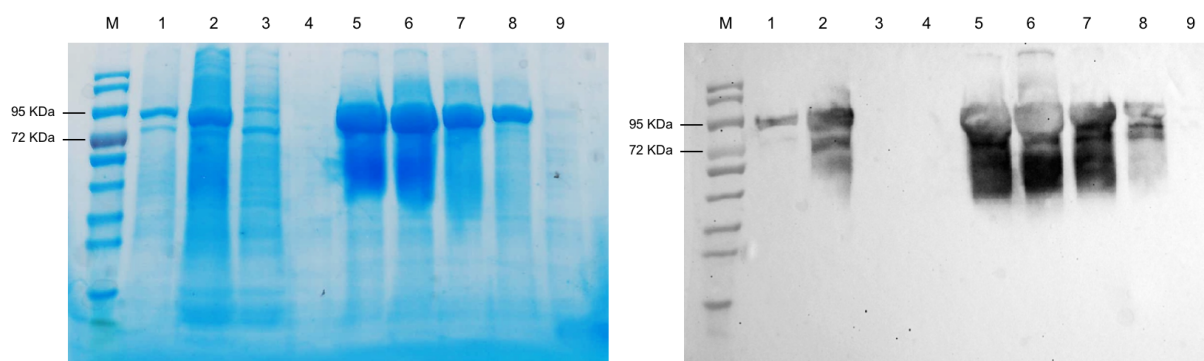
Figure 14 Assessment of Tras-VHH-R purification using Protein A affinity chromatography by SDS-PAGE (left) and Western-Blot (right). 1) Medium of cells secreting Tras-VHH-R. 2) Medium of cells secreting Tras-VHH-R concentrated by Amicon. 3) Flow-through of Tras-VHH-R medium – Fraction 1. 4) Column wash after Tras-VHH-R loading – Frac tion 2. 5) Fraction 16 of Tras-VHH-R elution. 6) Fraction 17 of Tras-VHH-R elution. 7) Fraction 18 of Tras-VHH-R elution. 8) Fraction 19 of Tras-VHH-R elution. 9) Column wash after Tras-VHH-R elution. M) Molecular weight marker.

By observation of bands presented at ~95 KDa on lanes 1, 2, 5, 6, 7 and 8 in the SDS-PAGE (Figure 14), it is possible to confirm the production of the antibody Tras-VHH-R by the cells and its successful purification by Protein A chromatography. Through Western-Blot technique, it is possible to confirm that the bands presented at ~95 KDa in SDS-PAGE correspond to the antibody Tras-VHH-R, using an anti-Human IgG HRP conjugated for detection of the Fc region in Tras-VHH-R.
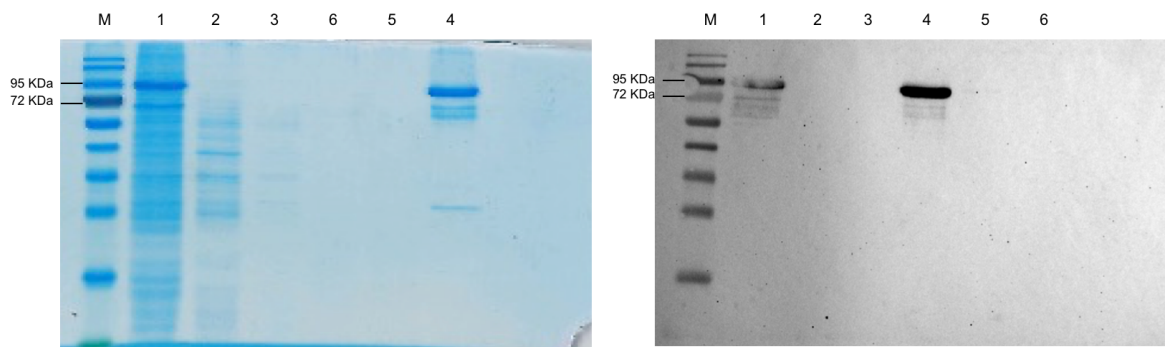
Figure 15 Assessment of Tras-VHH-R-H purification using Protein A affinity chromatography by SDS-PAGE (left) and Western-Blot (right). 1) Medium of cells secreting Tras-VHH-R. 2) Flow-through of Tras-VHH-R-H medium – Fraction 1. 3) Column wash after Tras-VHH-R-H loading – Fration 2. 4) Fraction 26 of Tras-VHH-R-H elution. 5) Fraction 27 of Tras-VHH-R-H elution. 6) Column wash after Tras-VHH-R-H elution. M) Molecular weight marker.

By observation of bands presented at ~95 KDa on lanes 1 and 4 in the SDS-PAGE (Figure 15), it is possible to confirm the production of the antibody Tras-VHH-R-H, by the cells and its successful purification by Protein A chromatography. Through Western-Blot technique, it is possible to confirm that the bands presented at ~95 KDa in SDS-PAGE correspond to the antibody Tras-VHH-R-H, using an anti-Human IgG HRP conjugated for detection of the Fc region in Tras-VHH-R-H.

According to the SDS-PAGE and Western-Blot performed to assess the purification of the three antibodies, the fractions containing the highest amount of antibody and therefore those chosen for the remaining experiments were: for Trastuzumab fractions 9 and 10; for Tras-VHH-R fractions 16, 17 and 18; for Tras-VHH-R-H fraction 26.

Before continuing with the pool of the respective fractions for antibody storage, due to the presence of other bands in both SDS-PAGE and Western-Blot of Trastuzumab (Figure 13) and Tras-VHH-R (Figure 14), which seem to correspond to some protein degradation and antibody complexes, an Amicon® Ultra device was used to clear antibody fractions. Fraction 9 and 10 of Trastuzumab were subjected to a centrifugation in a Amicon® Ultra 50K concentrator and fractions 16, 17 and 18 of Tras-VHH-R were subjected to a centrifugation in

a Amicon® Ultra 100K concentrator. After centrifugation, both concentrate and flow-through of each fraction were subjected to and SDS-PAGE gel. Concentrate of the centrifugation was also left incubating overnight at room temperature, to exclude the presence of proteases in these fractions.
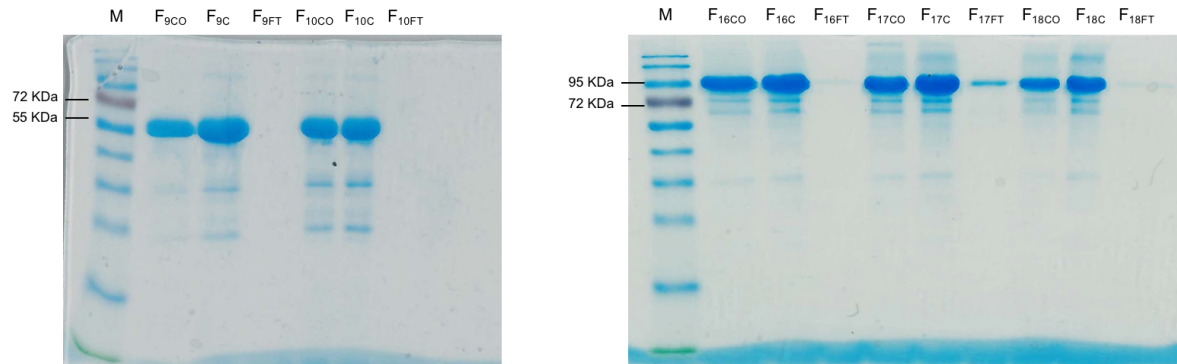
Figure 16 SDS-PAGE of Trastuzumab (left) and Tras-VHH-R (right) fractions after Amicon® Ultra device centrifugation. Concentrated (C) and concentrated left overnight (CO) samples (2 µL) were mixed with (23 µL) ddH2O and loading buffer (5 µL). Amicon flow-through (FT) sample (10 µL) was mixed with (15 µL) ddH2O and loading buffer (5 µL). M) Molecular weight marker.

According to the SDS-PAGE performed (Figure 16) with concentrated and concentrated left overnight fractions, the presence of proteases in these fractions can be dismiss, since both lanes present the same bands. Although the use of an Amicon® Ultra concentrator cleared the fractions of some contaminants SDS-PAGE still shows the presence of two bands below the band corresponding to Trastuzumab and Tras-VHH-R. To improve the purity of these fractions, it is necessary to add an additional chromatographic step, to eliminate the low molecular weight proteins (size exclusion chromatography). Since this was a preliminary experiment, the concentrated fractions were pooled and each antibody was diluted in PBS to a final concentration of 0.5 mg/mL and stored at 4 ºC.

3.3   Validation of antibody affinity towards Ricin A-chain

In order to assess the affinity of the purified antibodies that will be used for PIT construction an ELISA was performed. This technique is based on the binding of antibodies to target antigens absorbed in microplates. In this experiment, high binding microplates were coated with Ricin A-chain and subsequently antibodies were applied to the plate in different concentrations. The detection between sample antibodies and Ricin A-chain is made by using an anti-Human IgG HRP conjugated and the development by using TMB, absorbance was then measured at 450 nm in a Microplate Reader.
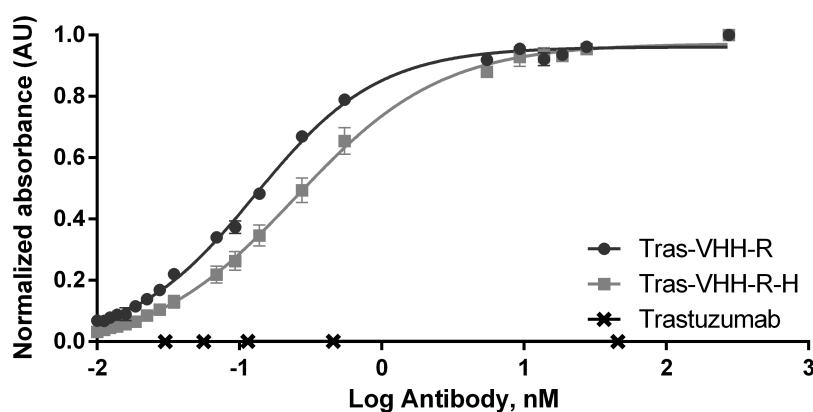
Figure 17 Assessment of antibodies relative affinity towards Ricin A-chain. To assess relative affinity of Trastuzumab, Tras-VHH-R and Tras-VHH-R-H, the antibodies (at indicated concentrations) were applied in duplicate to high bind microplates coated with Ricin A-chain (50ng/well). The EC50 values are defined as the antibody concentration (nM) that achieve half-maximal binding. The experiment is represented with error bars indicating SEM. The experiments were replicated two times.

Table 1 Values of EC50 of Tras-VHH-R and Tras-VHH-R-H and R-square of curve fit.

Antibody	EC_{50} (nM)	R-square
Tras-VHH-R	0.1289	0.9948
Tras-VHH-R-H	0.2478	0.9896

According to Figure 17 both antibodies Tras-VHH-R and Tras-VHH-R show similar affinity towards Ricin A-chain as it was expected, whereas Trastuzumab does not show any affinity, since this antibody is not composed with VHHs anti-Ricin A, serving as a negative control for this experiment. By the fitting of the sigmoid function to the results it was possible to obtain the EC_{50} values for each antibody, present in Table 1. The antibody Tras-VHH-R shows a higher relative affinity towards Ricin A-chain when compared to Tras-VHH-R-H.

3.4 Assessment of antibody specificity towards HER2

After confirming the affinity of the desired antibodies towards Ricin A-chain and before proceeding to cytotoxic assays with PIT against HER2$^+$ cell line, it is important to assess the specificity of the antibodies towards the HER2 receptor. For this, HER2$^+$ cell line SKBR3 was subjected to a flow cytometry assay. Cells were incubated with different concentrations of Trastuzumab, Tras-VHH-R and Tras-VHH-R-H. To better understand if Ricin A could disrupt or alter the interaction between the antibodies and the HER2 receptor, the incubation of the antibodies with the cells was made in the presence and absence of Ricin A. The HER2$^-$ cell line HeLa P4 was used as a negative control for this experiment and the incubation of Trastuzumab with SKBR3 cells was used as a positive control, since this antibody is known to target the HER2 receptor in breast cancer cells.
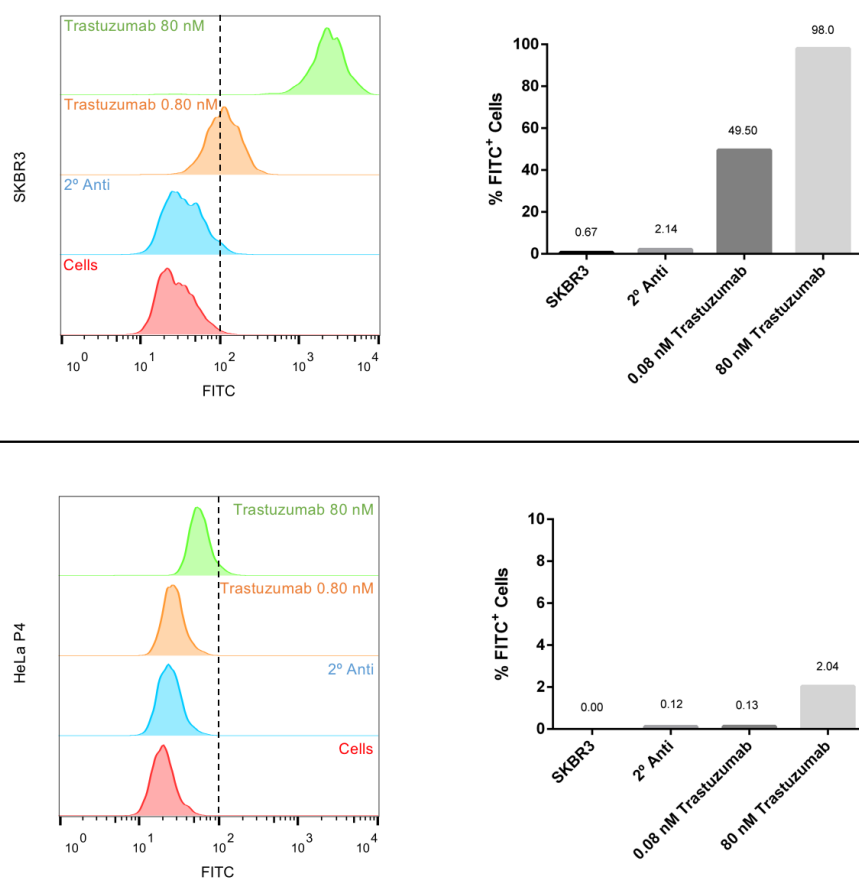
Figure 18 Assessment of Trastuzumab binding to HER2 receptor. SKBR3 and HeLa P4 cells (1x10^5) were incubated with different concentrations of Trastuzumab. After incubation, cells were immunostained with a secondary antibody (anti-Human IgG FITC-conjugated) for analyses of Trastuzumab binding through flow cytometry. Data recovered from flow cytometry was analysed with Flow Jo software.
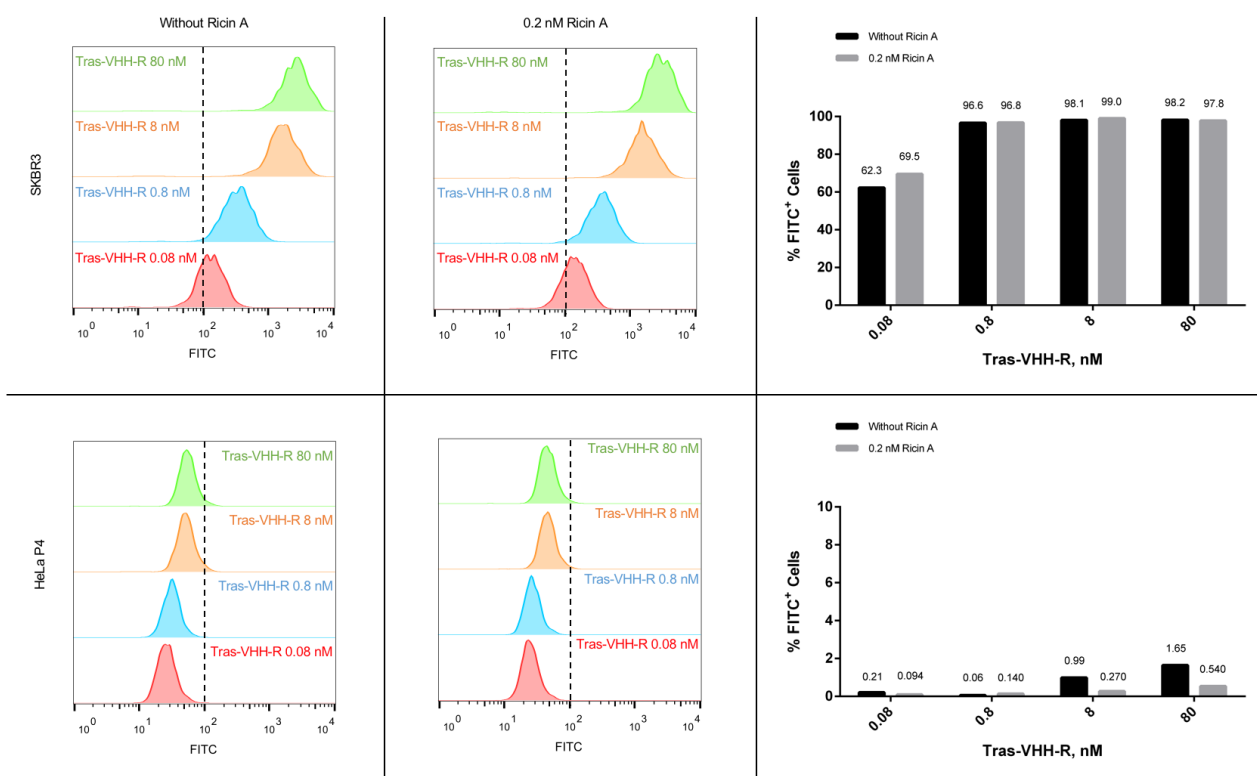
Figure 19 Assessment of Tras-VHH-R binding to HER2 receptor. SKBR3 and HeLa P4 cells ($1x10^5$) were incubated with different concentrations of Tras-VHH-R in presence (0.2 nM) or absence of Ricin A. After incubation, cells were immunostained with a secondary antibody (anti-Human IgG FITC-conjugated) for analyses of Tras-VHH-R binding through flow cytometry. Data recovered from flow cytometry was analysed with Flow Jo software.
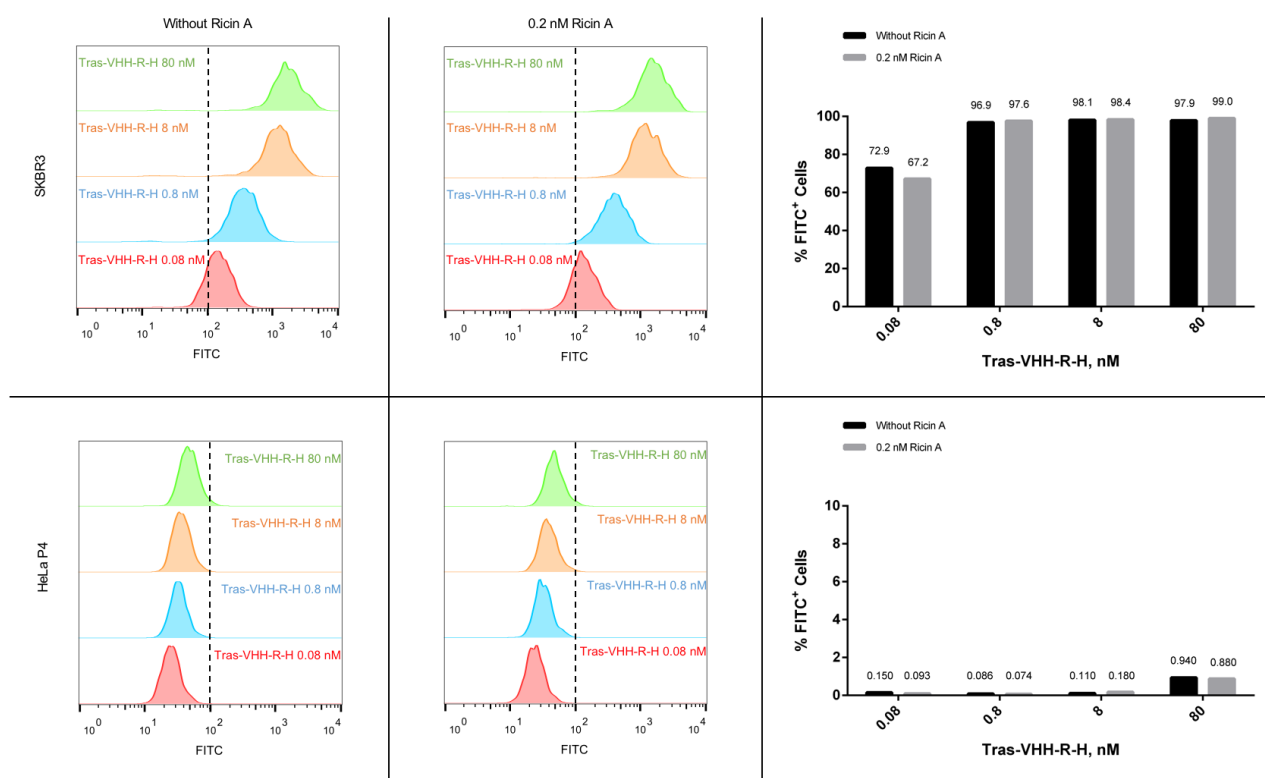
Figure 20 Assessment of Tras-VHH-R-H binding to HER2 receptor. SKBR3 and HeLa P4 cells (1×10^5) were incubated with different concentrations of Tras-VHH-R-H in presence (0.2 nM) or absence of Ricin A. After incubation, cells were immunostained with a secondary antibody (anti-Human IgG FITC-conjugated) for analyses of Tras-VHH-R binding through flow cytometry. Data recovered from flow cytometry was analysed with Flow Jo software.

As shown in Figure 18 Trastuzumab presented, has expected, binding against the HER2 receptor, with a 98 percentage of positive cells at the concentration of 80 nM. Both Tras-VHH-R (Figure 19) and Tras-VHH-R-H (Figure 20) show similar results as Trastuzumab, with a percentage of positive cells superior to 90 % for concentrations equal or superior of 0.8 nM. The incubation of the antibodies with cells in the presence of Ricin A show similar percentages of positive cells when compared with cells incubated with the antibodies.

The incubation of HeLa P4 cells with the antibodies in all conditions show a percentage of positive cells inferior to 3%, confirming the specificity of this antibodies towards the HER2 receptor.

3.5 PIT Cytotoxicity Assays in SBRR3 cell line

Finally, after assessing the affinity and specificity of antibodies that compose the PITs towards Ricin A and HER2, respectively, the cytotoxicity of the PITs was assessed by the colorimetric MTT assay. This assay is based on the capability of live cells to reduce MTT through the mitochondrial dehydrogenase activity leading to a formation of formazan compound with detectable UV spectrum. The MTT formazan compound gives a direct proportional measure of viable cells in culture.

Ricin A and the antibodies, Tras-VHH-R and Tras-VHH-R-H, were mixed in different concentrations of each of the compounds to produce PIT1 and PIT2, respectively. SKBR3 and HeLa P4 were incubated with the PITs for 48 and 72 h. Cells were also incubated with Ricin A, Tras-VHH-R and Tras-VHH-R-H alone. After incubation period, cell viability was assessed through MTT assay. All results are presented in percentage of cell viability, calculated based on the values of non-treated cells.
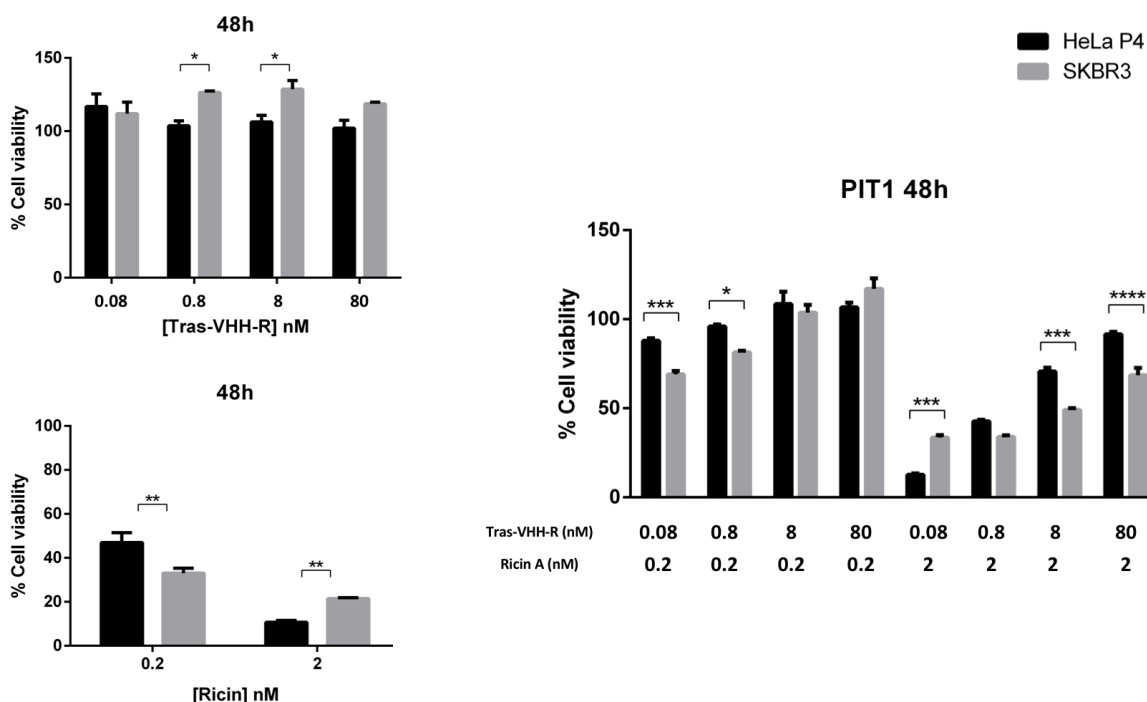
Figure 21 Effect of PIT 1, Ricin A and Tras-VHH-R in SKBR3 and HeLa P4 cell viability after 48 h of incubation. After incubation time, cells were washed and incubated with MTT (5 mg/mL) for 45 min. Formazan crystals were dissolved with DMSO, absorbance was measured at 490 nm in a Microplate Reader (BioRad, Model 680 Microplate Reader). Percentage of cell viability was determined through non-treated cells. Experiments were performed once in triplicate; error bars indicate SEM. Šidák-Holm test was performed to compare percentage of viability between SKBR3 and HeLa P4 cells in the same conditions
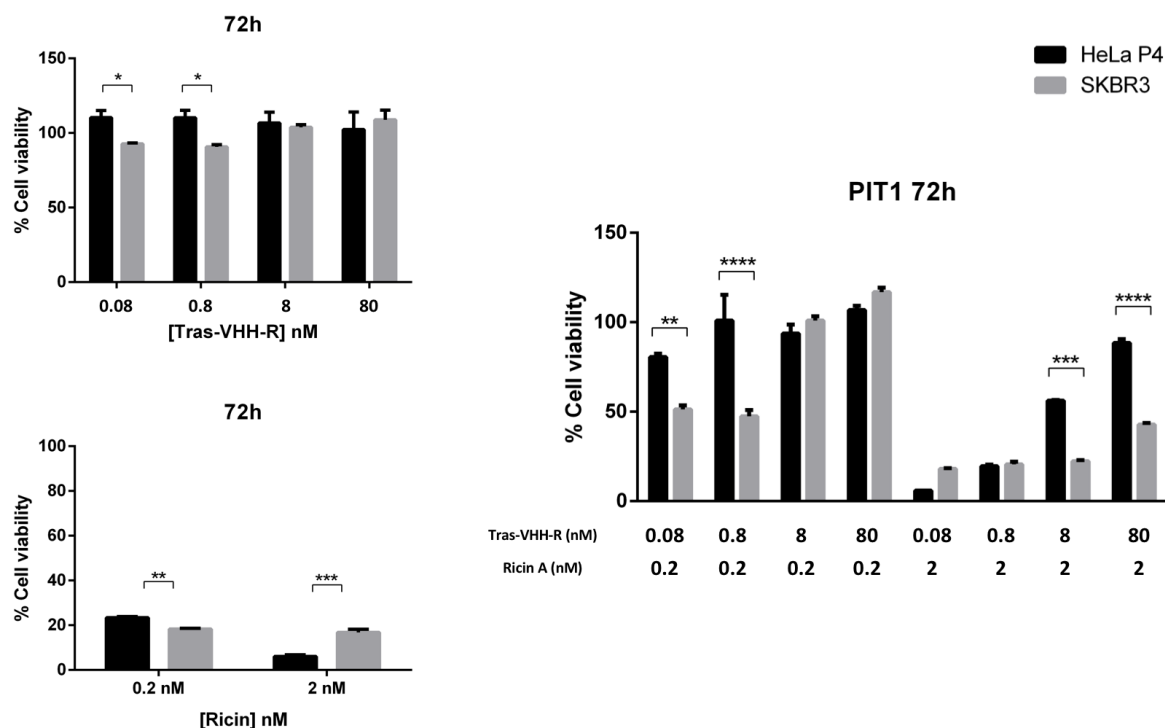
Figure 22 Effect of PIT 1, Ricin A and Tras-VHH-R in SKBR3 and HeLa P4 cell viability after 72 h of incubation. After incubation time, cells were washed and incubated with MTT (5 mg/mL) for 45 min. Formazan crystals were dissolved with DMSO, absorbance was measured at 490 nm in a Microplate Reader (BioRad, Model 680 Microplate Reader). Percentage of cell viability was determined through non-treated cells. Experiments were performed once in triplicate; error bars indicate SEM. Šidák-Holm test was performed to compare percentage of viability between SKBR3 and HeLa P4 cells in the same conditions

Figures 21 and 22 shows a significant reduced percentage of cell viability when cells are exposed to Ricin A for 48 and 72 h. Incubation with Tras-VHH-R shows significant decrease in cell viability of SKBR3 cells for both 48 and 72 h, with different antibody concentrations. Incubation with PIT1 shows significant decrease in cell viability of SKBR3 cells when compared with HeLa P4 for different concentrations of its components: 0.08 and 0.8 nM of Tras-VHH-R with 0.2 nM of Ricin A and 8 and 80 nM of Tras-VHH-R with 2 nM of Ricin A at 48 and 72 h.
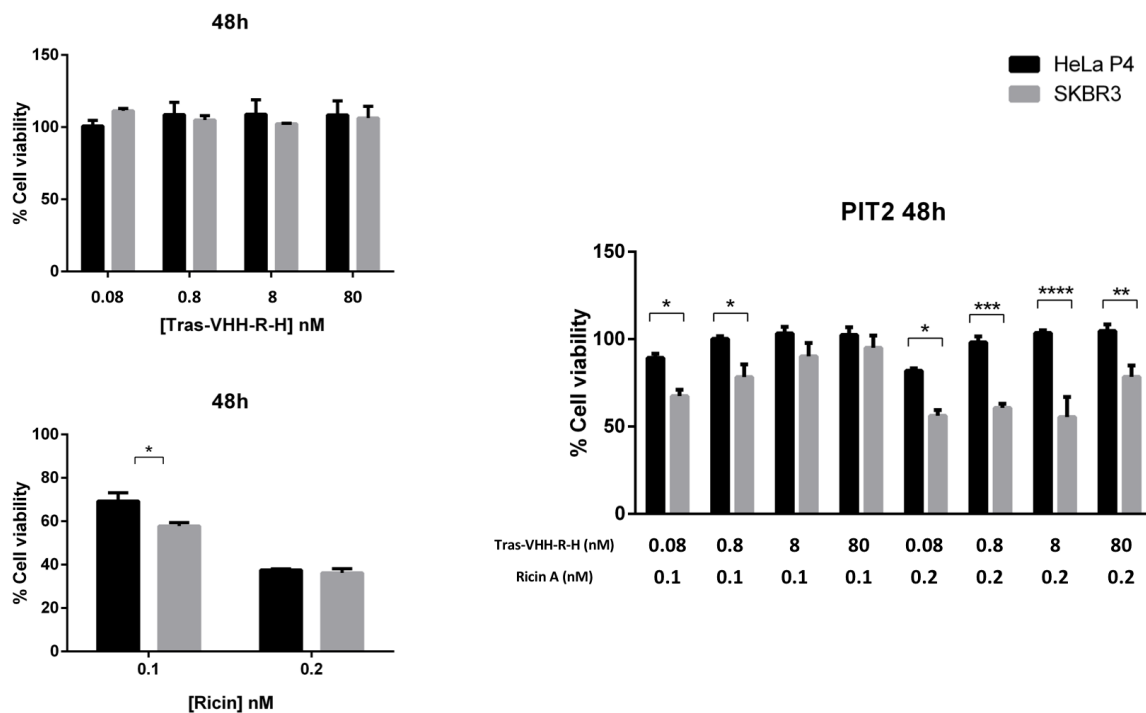
Figure 23 Effect of PIT 2, Ricin A and Tras-VHH-R-H in SKBR3 and HeLa P4 cell viability after 48 h of incubation. After incubation time, cells were washed and incubated with MTT (5 mg/mL) for 45 min. Formazan crystals were dissolved with DMSO, absorbance was measured at 490 nm in a Microplate Reader (BioRad, Model 680 Microplate Reader). Percentage of cell viability was determined through non-treated cells. Experiments were performed once in triplicate; error bars indicate SEM. Šidák-Holm test was performed to compare percentage of viability between SKBR3 and HeLa P4 cells in the same conditions
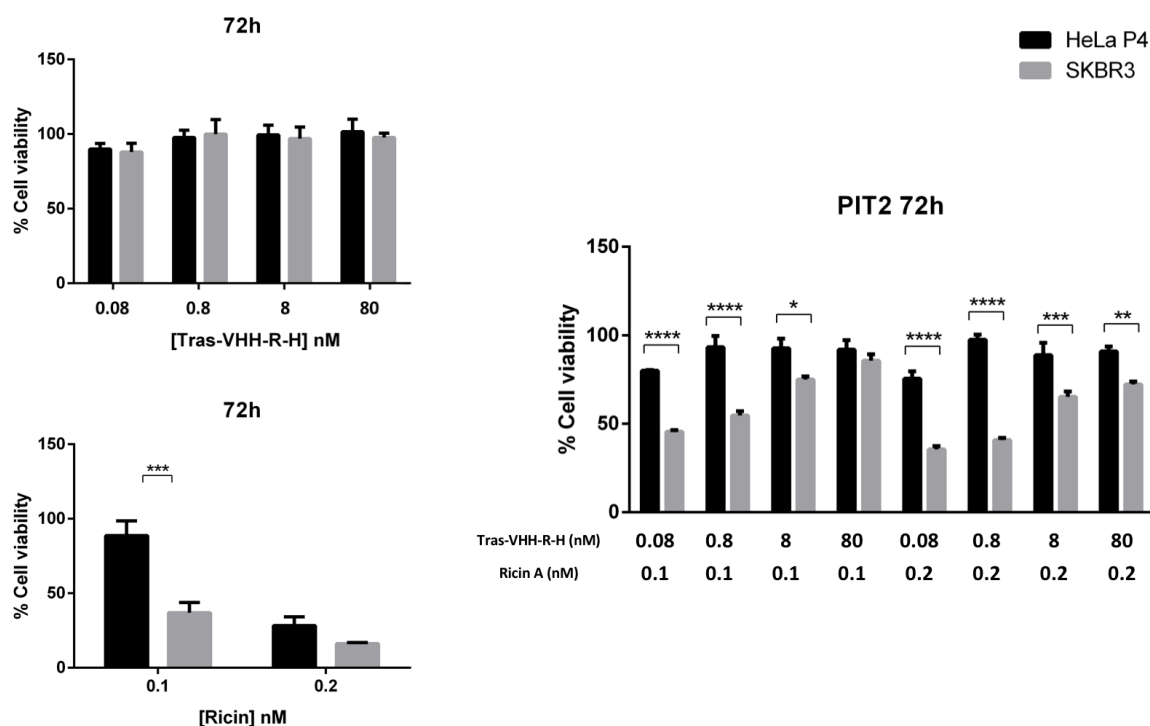
Figure 24 Effect of PIT 2, Ricin A and Tras-VHH-R-H in SKBR3 and HeLa P4 cell viability after 72 h of incubation. After incubation time, cells were washed and incubated with MTT (5 mg/mL) for 45 min. Formazan crystals were dissolved with DMSO, absorbance was measured at 490 nm in a Microplate Reader (BioRad, Model 680 Microplate Reader). Percentage of cell viability was determined through non-treated cells. Experiments were performed once in triplicate; error bars indicate SEM. Šidák-Holm test was performed to compare percentage of viability between SKBR3 and HeLa P4 cells in the same conditions

Figures 23 and 24 shows a significant reduced percentage of cell viability when cells are exposed to Ricin A for 48 and 72 h. Incubation with Tras-VHH-R-H shows no significant decrease in cell viability of SKBR3 and HeLa P4 cells for both 48 and 72 h. Incubation with PIT2 shows significant decrease in cell viability of SKBR3 cells when compared with HeLa P4 for different concentrations of its components: 0.08 and 0.8 nM of Tras-VHH-R-H with 0.1 nM of Ricin A and 0.08, 0.8, 8 and 80 nM of Tras-VHH-R with 0.2 nM at 48 h; 0.08, 0.8 and 8 nM of Tras-VHH-R-H with 0.1 nM of Ricin A and 0.08, 0.8, 8 and 80 nM of Tras-VHH-R with 0.2 nM at 72 h.
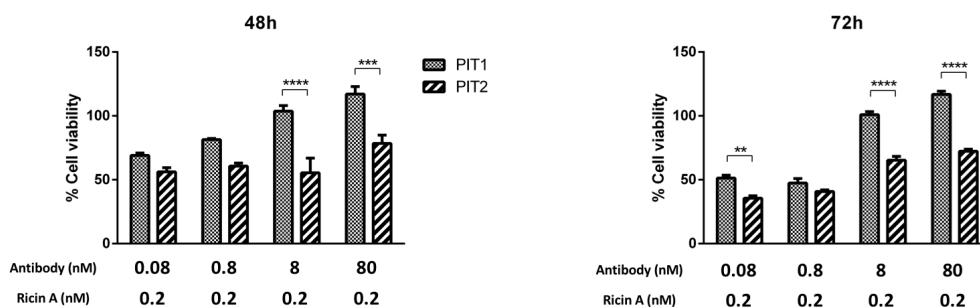
Figure 25 Effect of PIT 1and PIT2 in SKBR3 cell viability after 48 and 72 h of incubation. After incubation time, cells were washed and incubated with MTT (5 mg/mL) for 45 min. Formazan crystals were dissolved with DMSO, absorbance was measured at 490 nm in a Microplate Reader (BioRad, Model 680 Microplate Reader). Percentage of cell viability was determined through non-treated cells. Experiments were performed once in triplicate; error bars indicate SEM. Šidák-Holm test was performed to compare percentage of viability between SKBR3 and HeLa P4 cells in the same conditions.

Figure 25 compares the percentage of cell viability between PIT1 and PIT2 in SKBR3 cell line at 48 h and 72 h, and shows a significant decrease in cell viability for SKBR3 cells treated with PIT2 when compared to cells treated with PIT1 at antibody concentrations of 8 and 80 nM at 48 h and 0.08, 8 and 80 nM at 72h.
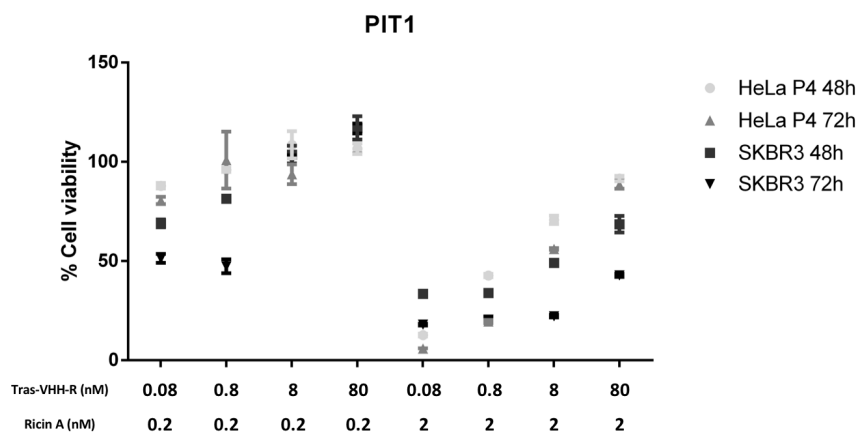
Figure 26 Effect of PIT 1 in HeLa P4 and SKBR3 cell viability after 48 and 72 h of incubation. After incubation time, cells were washed and incubated with MTT (5 mg/mL) for 45 min. Formazan crystals were dissolved with DMSO, absorbance was measured at 490 nm in a Microplate Reader (BioRad, Model 680 Microplate Reader). Percentage of cell viability was determined through non-treated cells. Experiments were performed once in triplicate; error bars indicate SEM.
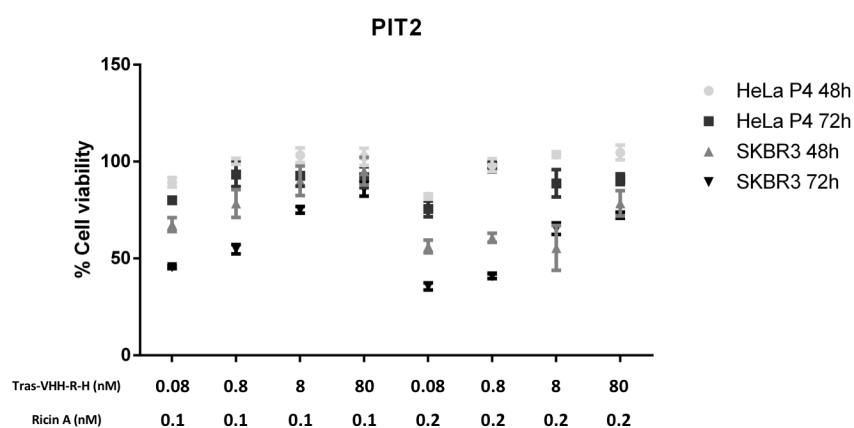
Figure 27 Effect of PIT 1 in HeLa P4 and SKBR3 cell viability after 48 and 72 h of incubation. After incubation time, cells were washed and incubated with MTT (5 mg/mL) for 45 min. Formazan crystals were dissolved with DMSO, absorbance was measured at 490 nm in a Microplate Reader (BioRad, Model 680 Microplate Reader). Percentage of cell viability was determined through non-treated cells. Experiments were performed once in triplicate; error bars indicate SEM.

Figures 26 and 27 allow a comparison of the effect of PIT1 and PIT2, respectively, in HeLa P4 and SKBR3 cell lines between the 48 h and 72 h incubation period. Both figures show an accentuated decrease of cell viability at 72h, which is more visible at the SKBR3 cell line of that in HeLa P4 cell line.

4.   Discussion

This project began with the transfection of HEK293T cells with the plasmids encoding for Trastuzumab and the antibodies which compose the PITs, Tras-VHH-R and Tras-VHH-R-H, for ensuring protein expression and secretion, which made this a vital step before continuing with their large scale production.

To confirm protein expression and secretion in these cells, Western-Blot analyses was performed, revealing the presence of the desired antibodies, has shown in Figure 9. The bands with higher intensity correspond to wells transfected with 1.5 µg of DNA, corroborating the change in colour media and cell density, observed in Figure 8. With this first step, it was possible to confirm the expression and secretion of the desired antibodies, Trastuzumab, Tras-VHH-R and Tras-VHH-R-H, in mammalian cells, but also possible to understand that cells are susceptible to high DNA quantities in the transfection process. These high quantities lead to low cell viability, reducing the amount of protein production and secretion.

With the results obtained by the transfection of HEK293T cells it was possible to establish a protocol for the large scale production of antibodies in mammalian cells. FreeStyle™ 293-F cells were chosen due to their capacity of transfection in high volumes and cell density. Cells were transfected with less than half of the DNA used per cell in HEK293T, to ensure cell viability.

To proceed with the purification of antibodies produced by 293-F cells, a Protein A affinity chromatography was performed. This technique allows the isolation of antibodies or antibody fragments composed of an Fc portion which have high affinity to protein A.

The different phases of antibody purification can be followed through the measurement of absorbance and conductivity. In the chromatograms of Figures 10, 11 and 12, which correspond to the purification of the antibodies Trastuzumab, Tras-VHH-R and Tras-VHH-R-H, respectively, it is possible to observe two distinct peaks. The first corresponds to the flow through, the moment of sample injection in the column, here all proteins with no affinity to the column are eluted increasing the absorbance read at 280_{nm}; and the second corresponds to the elution of proteins with affinity to the column due to pH decrease. This is consistent with a decrease of conductivity due to the introduction of the elution buffer in the column, which is explained by the absence of salts in its constitution. Therefore, the antibodies of interest must be present in the fractions corresponding to the second peak. For Trastuzumab the second peak corresponds to fractions 8 to 12, for Tras-VHH-R 14 to 21 and for Tras-VHH-R-H fraction 26. It is important to mention that it was difficult to obtain a correct baseline of absorbance during the three chromatographies which

can be observe in the chromatograms. To better understand if the purification was successfully performed, it is necessary the coupling of the chromatograms results with SDS-PAGE and Western-Blot analyses.

SDS-PAGE and Western-Blot confirmed the presence of the desired antibodies in cell medium and elution fractions chosen by absorbance at 280_{nm} (Figure 13, 14 and 15). Fractions corresponding to the flow through of chromatography showed no presence of the bands corresponding to the produced antibodies, confirming that all had bound to the column and were eluted with pH exchange.

Although large scale production and purification by protein A chromatography have shown to be efficient, the SDS-PAGE performed showed that other proteins have co-eluted with Trastuzumab and Tras-VHH-R. Western-Blot allowed the identification of antibodies or antibody fragments containing a Fc region present in all analysed fractions, showing bands corresponding to the antibody Trastuzumab, Tras-VHH-R and also bands with higher and lower molecular mass than the expected ones.

With these results, it is possible to conclude that the other proteins that have co-eluted with the antibodies of interest are most likely antibody complexes or fragments of its degradation, since FreeStyle™ 293-F is derived from an embryonic kidney cell line that does not produce antibodies. With the intention to clear the eluted fractions and to exclude the presence of proteases present in the elution fractions, which might be responsible for the low molecular mass bands in the SDS-PAGE and the Western-Blot (Figure 13 and 14) an Amicon® Ultra device was used.

All fractions of Amicon® centrifugation and fractions left overnight were subjected to an SDS-PAGE. As it can be observed in Figure 16 no significant changes were visible in lanes correspondent to the fractions left overnight, rejecting the possibility of proteases in these fractions, making it more probable that protein degradation occurred during antibody production. Amicon® centrifugation was not able to clear these fractions from all additional bands, so to improve the efficiency of purification, a size-exclusion chromatography should be coupled to this process, or to ensure no antibody degradation, time of antibody production by transfected 293-F cells could be reduced.

In the future, production time will be lower and to improve antibody purification a size-exclusion chromatography could be performed after the protein A chromatography, therefore ensuring higher antibody purity and also allowing the confirmation of antibody degradation during production. The results obtained from this antibody production and purification were sufficient to continue with the assessment of antibody affinity towards Ricin A–chain.

The antibodies Trastuzumab, Tras-VHH-R and Tras-VHH-R-H were tested in an ELISA assay to assess their binding towards Ricin A-chain. The EC_{50} is defined as the dose at which 50 % of the maximum effect is produced or the concentration of drug at which the drug is half-maximally effective [58]. In this case it indicates the concentration of antibody required for 50 % maximal Ricin A binding in ELISA.

According to the results presented in Table 1, the curve fits the results obtained by ELISA (Table 1) and EC_{50} values attained for sigmoid curve adjustment fully represent the binding capability of the antibodies. According to Figure 17, Trastuzumab showed no affinity towards Ricin A, since there is no VHH targeting this protein. Tras-VHH-R and Tras-VHH-R-H showed high affinity towards Ricin A has observed by their EC_{50} values (Table 1). However, Tras-VHH-R shows a lower EC_{50} when compared to Tras-VHH-R-H, suggesting a higher affinity towards Ricin A, which can be explained by the number of anti-Ricin A VHHs presented in their constitution.

When comparing the values obtained in this experiments with the EC_{50} values of the VHH anti-Ricin A (RTA-D10, $EC_{50}\approx0.66$ nM) [53] alone, it is possible to notice an increase in these values, suggesting a decrease in affinity when the VHH is dimerized and coupled to a scFv-Fc Trastuzumab. Nonetheless, values obtained are in the same binding range of the VHH alone and the alteration can be explained by the adaptation of the VHH binding capability when coupled to a much bigger molecule and another VHH, which can hinder the binding to Ricin A thus decreasing the affinity towards this protein.

Although the anti-Ricin A VHH decreased its affinity when coupled, it could still efficiently bind to Ricin A, therefore the assessment of Tras-VHH-R and Tras-VHH-R-H binding to HER2 was initiated.

Before continuing with PIT cytotoxicity assays, it was important to assess antibody specificity towards the HER2 receptor. For this, a flow cytometry assay was performed. Both HER2$^+$ (SBKR3) and HER2$^-$ (HeLa P4) cells where incubated with antibodies Trastuzumab, Tras-VHH-R and Tras-VHH-R-H. To better assess if the binding of Ricin A to the VHHs present in the antibodies could alter their binding to the HER2 receptor, cells were also incubated with Ricin A at 0.2 nM and Tras-VHH-R or Tras-VHH-R-H.

Trastuzumab antibody served as positive control for this experience since it is known to bind to the HER2 receptor. According to Figure 18, Trastuzumab binds to HER2 showing a percentage of positive stained cells of 49.50 % and 98 % at concentrations 0.80 and 80 nM, respectively, suggesting that an antibody concentration of 0.80 nM is not enough antibody to saturate every cell. Similar results were acquired for antibodies Tras-VHH-R and Tras-VHH-R-H (Figures 19 and 20), both antibodies show an increase in the percentage of positive

stained cells from concentration 0.08 to 80 nM. No visible changes were observed when Ricin A was added to the antibodies Tras-VHH-R and Tras-VHH-R-H and incubated with the cells, confirming that binding of Ricin A to the antibodies does not affect their binding to the HER2 receptor. In figures 18, 19 and 20 it is possible to observes that neither Trastuzumab, Tras-VHH-R and Tras-VHH-R-H respectively, bind to the HER2⁻ cell line HeLa P4, showing percentages of positive stained cells lower than 2 %, confirming the specificity of this antibodies towards the HER2 receptor.

The specific binding of anti-HER2 VHH used in the Tras-VHH-R-H construction was not assessed in a flow cytometry assay. However, previous studies showed high affinity of this VHH towards the HER2 receptor, when used in a similar construction (Fc-FITC-VHH-HER2) (data not shown).

Ultimately, assays of cytotoxicity were performed with PIT 1 and 2, to assess if this new type of immunotoxins could efficiently kill HER2⁺ cells while protecting HER2⁻ cells. For this SKBR3 and HeLa P4 cells were incubated with Ricin A, Tras-VHH-R, Tras-VHH-R-H, PIT1 and PIT2, for 48 and 72h. To assess the best concentration for PIT construction, both PIT1 and PIT2 were incubated with different concentration of antibody and Ricin A.

According to Figure 21 and 22 PIT1 could reduce cell viability in HER2⁺ cells (SKBR3) but still retaining a percentage of viable cells near or at 100 % in HER2⁻ cells (HeLa P4) (0.08 and 0.8 nM Tras-VHH-R plus 0.2 nM Ricin A; 80 nM Tras-VHH-R plus 0.2 nM Ricin A).

The incubation of these cells with Ricin A at 0.2 and 2 nM produced a visible decrease in cell viability in both cell lines, which does not happen with the concentrations showed above for the incubation of HeLa P4 with PIT1; indicating that the decrease of cell viability observed in SKBR3 cells is due to the internalization of PIT1 and not due to free Ricin A present in the cell medium.

At concentrations of 8 and 80 nM of Tras-VHH-R with 0.2 nM of Ricin A no visible changes in cell viability were observed between SKBR3 and HeLa P4 cells. The most likely reason why this happened is an excess of antibody when compared to Ricin A, leading to a competition between Tras-VHH-R and PIT1, where Tras-VHH-R is in a much higher concentration than PIT1.

If we compare the cell viability of SKBR3 cells when incubated with PIT1 at 48h and 72 h (Figure 26) for the most efficient concentrations (0.08 and 0.8 nM Tras-VHH-R plus 0.2 nM Ricin A; 80 nM Tras-VHH-R plus 0.2 nM Ricin A), an evident decrease in cell viability can be observed which suggests a prolong cytotoxic effect of this PIT.

Regarding PIT2, because of the reduced number of anti-Ricin A VHHs present in Tras-VHH-R-H when compared to Tras-VHH-R-H, the concentrations of Ricin A used for

PIT2 is lower than those used for PIT1. PIT2 shows promising results, having a variety of concentrations at which percentage of cell viability is lower than 70 % for SKBR3 cell line and near or 100 % for HeLa P4 cell line (0.8 nM Tras-VHH-R-H plus 0.1 nM Ricin a; 0.8, 8 and 80 nM Tras-VHH-R-H plus 0.2 nM Ricin A) (Figures 23 and 24). As happened with PIT1, the reduction of cell viability in SKBR3 incubated with PIT2 is due to its internalization and not because of free Ricin A in the cell medium. With PIT2 a prolong cytotoxic effect was too observed by the comparison of its effect at 48 and 72 h (Figure 27), at the concentrations listed above.

The purpose of constructing PIT2 was to enhance PIT internalization applying the concepts of Moody, P. R. *et al.*, but instead of using streptavidin to cross-link the receptors and trigger endocytosis, the antibody Tras-VHH-R-H was constructed to have two different binding sites to the receptor HER2, one in the scFv portion of Trastuzumab and the other on the VHH added to end of the antibody.

By comparing the percentage of cell viability in SKBR3 cells incubated with PIT1 and cells incubated with PIT2 in Figure 25, it is possible to observe significant alteration in the percentage of cell viability at both 48 and 72 h. The comparison between the two PITs was made at the same concentrations, indicating that the reduction of cell viability observed with PIT2 when compared with PIT1 may be due to an enhanced internalization of the antibody.

Although this research shows great promise in the advancement of immunotoxins and also in the discovery of a new method to trigger endocytosis in a variety of targeted therapies, further experiments are needed to better understand the internalization of these PITs. Future work will include flow cytometry internalization assays and also confocal microscopy to analyse the journey of the PITs inside the cell and also its interaction with cell membrane. A surface plasmon resonance (SPR) will also be performed to better understand the binding of Ricin A to the PITs and also determine the best concentration for PIT construction.

5.   Conclusion

In 2018 is estimated that there will be 266,120 new cases of breast cancer in females, making it 30% of all new diagnosis in cancer for women. From these new cases, approximately 53,224 will be breast cancer HER2$^+$, in the United States of America alone. This worrying number of new cases makes it imperative to find new therapeutics for this disease but also to improve the existing ones.

With this project, we tried to improve the toxicity of Trastuzumab by coupling it with a toxin, Ricin A, in an innovative type of immunotoxin. We verified that PIT1 is able to deliver Ricin A to the HER2$^+$ cell line, SKBR3, but still protecting the HER2$^-$ cell line, HeLa P4. With the construction of PIT1, it was envisioned a way to enhance its internalization and therefore the delivery of Ricin A, by introducing new binding site to HER2. This new proimmunotoxin (PIT2) also showed the capability of diminish cell viability in SKBR3 cells while maintaining the protection towards HeLa P4 cells. When comparing these two constructions in the same conditions, PIT2 showed higher cytotoxicity than PIT1, leading us to think that this new mechanism of HER2 binding enhances its internalization.

In the future, to better understand the journey of the PIT inside the cell and its interaction with the cell membrane, flow cytometry internalization assays and also confocal microscopy will be performed. To determine the best concentration for PIT construction an SPR analyses will be executed. It will be of the most importance to initiate testing of this biopharmaceutical in Trastuzumab resistant cell lines, to enable its use in the largest possible group of patients.

What makes the proimmunotoxin concept so interesting is the possibility of being applied to a large spectrum of antibodies and toxins, but also to the transportation of pharmaceuticals. We hope that this work will contribute for the advance in the production of new and more potent biopharmaceuticals against breast cancer.

6. References

1. Thorpe, P. E. *et al.* Toxicity of diphteria toxin for lymphoblastoid cells is increased by conjugation to antilymphocytic globulin. *Nature* **271,** 752–755 (1978).

2. Alewine, C., Hassan, R. & Pastan, I. Advances in Anticancer Immunotoxin Therapy. *Oncologist* **20,** 176–185 (2015).

3. Olsen, E. *et al.* Pivotal phase III trial of two dose levels of denileukin diftitox for the treatment of cutaneous T-cell lymphoma. *J Clin Oncol* **19,** 376–388 (2001).

4. Wayne, A. S., FitzGerald, D. J., Kreitman, R. J. & Pastan, I. Immunotoxins for leukemia. *Blood* **123,** 2470–2477 (2014).

5. Antignani, A. & FitzGerald, D. Immunotoxins: The role of the toxin. *Toxins* **5,** 1486–1502 (2013).

6. Chaudhary, V. K. *et al.* A recombinant immunotoxin consisting of two antibody variable domains fused to Pseudomonas exotoxin. *Nature* **339,** 394–7 (1989).

7. Du, X., Beers, R., FitzGerald, D. J. & Pastan, I. Differential cellular internalization of anti-CD19 and -CD22 immunotoxins results in different cytotoxic activity. *Cancer Res.* **68,** 6300–6305 (2008).

8. Jilani, I. *et al.* Differences in CD33 intensity between various myeloid neoplasms. *Am. J. Clin. Pathol.* **118,** 560–566 (2002).

9. Peters, C. & Brown, S. Antibody-drug conjugates as novel anti-cancer chemotherapeutics. *Biosci. Rep.* **35,** e00225 (2015).

10. Michalska, M., Schultze-seemann, S., Bogatyreva, L., Wetterauer, U. & Wolf, P. *In vitro* and *in vivo* effects of a recombinant anti-PSMA immunotoxin in combination with docetaxel against prostate cancer. *Oncotarget* **7,** (2014).

11. Zhang, F. *et al.* An Anti-PSMA Bivalent Immunotoxin Exhibits Specificity and Efficacy for Prostate Cancer Imaging and Therapy. *Adv. Healthc. Mater.* **2,** 736–744 (2013).

12. Cao, Y. *et al.* Design optimization and characterization of Her2/neu-targeted immunotoxins: comparative in vitro and in vivo efficacy studies. *Oncogene* **33,** 429–439 (2014).

13. Bühler, P. *et al.* Influence of structural variations on biological activity of anti-PSMA scFv and immunotoxins targeting prostate cancer. *Anticancer Res.* **30,** 3373–3379 (2010).

14. Nelson, A. L. Antibody fragments: Hope and hype. *mAbs* **2,** 77–83 (2010).

15. Chames, P., Van Regenmortel, M., Weiss, E. & Baty, D. Therapeutic antibodies: Successes, limitations and hopes for the future. *British Journal of Pharmacology* **157,**

220–233 (2009).

16.   Shan, L., Liu, Y. & Wang, P. Recombinant Immunotoxin Therapy of Solid Tumors: Challenges and Strategies. *J. Basic Clin. Med.* **2,** 1–6 (2013).

17.   Arbabi Ghahroudi, M., Desmyter, A., Wyns, L., Hamers, R. & Muyldermans, S. Selection and identification of single domain antibody fragments from camel heavy-chain antibodies. *FEBS Lett.* **414,** 521–526 (1997).

18.   Arbabi-Ghahroudi, M. Camelid single-domain antibodies: Historical perspective and future outlook. *Front. Immunol.* **8,** (2017).

19.   Audi, J., Belson, M., Patel, M., Schier, J. & Osterloh, J. Ricin poisoning: A comprehensive review. *JAMA* **294,** 2342–2351 (2005).

20.   Słomińska-Wojewódzka, M. & Sandvig, K. Ricin and Ricin-Containing Immunotoxins: Insights into Intracellular Transport and Mechanism of action in Vitro. *Antibodies* **2,** 236–269 (2013).

21.   Hartley, M. R. & Lord, J. M. Cytotoxic ribosome-inactivating lectins from plants. *Biochimica et Biophysica Acta - Proteins and Proteomics* **1701,** 1–14 (2004).

22.   Olsnes, S., Refsnes, K. & Pihl, A. Mechanism of action of the toxic lectins abrin and ricin. *Nature* **249,** 627–631 (1974).

23.   Van Deurs, B. *et al.* Estimation of the amount of internalized ricin that reaches the trans-Golgi network. *J. Cell Biol.* **106,** 253–267 (1988).

24.   van Deurs, B., Tønnessen, T. I., Petersen, O. W., Sandvig, K. & Olsnes, S. Routing of internalized ricin and ricin conjugates to the Golgi complex. *J. Cell Biol.* **102,** 37–47 (1986).

25.   Wu, Y. H., Shih, S. F. & Lin, J. Y. Ricin Triggers Apoptotic Morphological Changes through Caspase-3 Cleavage of BAT3. *J. Biol. Chem.* **279,** 19264–19275 (2004).

26.   Rao, P. V *et al.* in *Biochem Pharmacol* **69,** 855–865 (2005).

27.   Williams, J. M. *et al.* Comparison of ribosome-inactivating proteins in the induction of apoptosis. *Toxicol. Lett.* **91,** 121–127 (1997).

28.   Komatsu, N., Oda, T. & Muramatsu, T. Involvement of both caspase-like proteases and serine proteases in apoptotic cell death induced by ricin, modeccin, diphtheria toxin, and Pseudomonas toxin. *J. Biochem.* **124,** 1038–1044 (1998).

29.   Zhou, X. X., Ji, F., Zhao, J. L., Cheng, L. F. & Xu, C. F. Anti-cancer activity of anti-p185HER-2 ricin A chain immunotoxin on gastric cancer cells. *J. Gastroenterol. Hepatol.* **25,** 1266–1275 (2010).

30.   Erickson, H. K. *et al.* Antibody-maytansinoid conjugates are activated in targeted cancer cells by lysosomal degradation and linker-dependent intracellular processing.

Cancer Res. **66,** 4426–4433 (2006).

31.   Weldon, J. E. *et al.* A protease-resistant immunotoxin against CD22 with greatly increased activity against CLL and diminished animal toxicity. *Blood* **113,** 3792–3800 (2009).

32.   McKee, M. L. & FitzGerald, D. J. Reduction of furin-nicked Pseudomonas exotoxin A: An unfolding story. *Biochemistry* **38,** 16507–16513 (1999).

33.   Chiron, M. F., Ogata, M. & FitzGerald, D. J. Pseudomonas exotoxin exhibits increased sensitivity to furin when sequences at the cleavage site are mutated to resemble the arginine-rich loop of diphtheria toxin. *Mol. Microbiol.* **22,** 769–78 (1996).

34.   Wilson, B. a & Collier, R. J. Diphtheria toxin and Pseudomonas aeruginosa exotoxin A: active-site structure and enzymic mechanism. *Curr. Top. Microbiol. Immunol.* **175,** 27–41 (1992).

35.   Lord, J. M., Roberts, L. M. & Robertus, J. D. Ricin: structure, mode of action, and some current applications. *FASEB J* **8,** 201–208 (1994).

36.   Moreau, D. *et al.* Genome-Wide RNAi Screens Identify Genes Required for Ricin and PE Intoxications. *Dev. Cell* **21,** 231–244 (2011).

37.   Pirie, C. M., Hackel, B. J., Rosenblum, M. G. & Wittrup, K. D. Convergent potency of internalized gelonin immunotoxins across varied cell lines, antigens, and targeting moieties. *J. Biol. Chem.* **286,** 4165–4172 (2011).

38.   Ogata, M., Chaudhary, V. K., Pastan, I. & FitzGerald, D. J. Processing of Pseudomonas exotoxin by a cellular protease results in the generation of a 37,000-Da toxin fragment that is translocated to the cytosol. *J. Biol. Chem.* **265,** 20678–20685 (1990).

39.   Yamaizumi, M., Mekada, E., Uchida, T. & Okada, Y. One molecule of diphtheria toxin fragment a introduced into a cell can kill the cell. *Cell* **15,** 245–250 (1978).

40.   DeSantis, C. E., Ma, J., Goding Sauer, A., Newman, L. A. & Jemal, A. Breast cancer statistics, 2017, racial disparity in mortality by state. *CA. Cancer J. Clin.* (2017). doi:10.3322/caac.21412

41.   American Cancer Society. Cancer Facts & Figures 2018. *Am. Cancer Soc.* 28–43 (2018). doi:10.1182/blood-2015-12-687814

42.   Alteri, R. et al. *Breast Cancer Facts & Figures 2017-2018. American Cancer Society* (2017).

43.   Yarden, Y. Biology of HER2 and its importance in breast cancer. in *Oncology* **61,** 1–13 (2001).

44.   Klapper, L. N., Kirschbaum, M. H., Sela, M. & Yarden, Y. Biochemical and clinical

implications of the ErbB/HER signaling network of growth factor receptors. *Adv. Cancer Res.* **77,** 25–79 (2000).

45. Ahmed, S., Sami, A. & Xiang, J. HER2-directed therapy: current treatment options for HER2-positive breast cancer. *Breast Cancer* **22,** 101–116 (2015).

46. Hudis, C. A. Trastuzumab — Mechanism of Action and Use in Clinical Practice. *N. Engl. J. Med.* **357,** 39–51 (2007).

47. Molina, M. A. *et al.* Trastuzumab (Herceptin), a humanized anti-HER2 receptor monoclonal antibody, inhibits basal and activated HER2 ectodomain cleavage in breast cancer cells. *Cancer Res.* **61,** 4744–4749 (2001).

48. Junttila, T. T. *et al.* Ligand-Independent HER2/HER3/PI3K Complex Is Disrupted by Trastuzumab and Is Effectively Inhibited by the PI3K Inhibitor GDC-0941. *Cancer Cell* **15,** 429–440 (2009).

49. Arnould, L. *et al.* Trastuzumab-based treatment of HER2-positive breast cancer: An antibody-dependent cellular cytotoxicity mechanism? *Br. J. Cancer* **94,** 259–267 (2006).

50. Bertelsen, V. & Stang, E. The mysterious ways of ErbB2/HER2 trafficking. *Membranes* **4,** 424–446 (2014).

51. Klapper, L. N., Waterman, H., Sela, M. & Yarden, Y. Tumor-inhibitory antibodies to HER-2/ErbB-2 may act by recruiting c-Cbl and enhancing ubiquitination of HER-2. *Cancer Res.* **60,** 3384–3388 (2000).

52. Moody, P. R. *et al.* Receptor Crosslinking: A General Method to Trigger Internalization and Lysosomal Targeting of Therapeutic Receptor:Ligand Complexes. *Mol. Ther.* **23,** 1888–1898 (2015).

53. Vance, D. J., Tremblay, J. M., Mantis, N. J. & Shoemaker, C. B. Stepwise engineering of heterodimeric single domain camelid VHH antibodies that passively protect mice from ricin toxin. *J. Biol. Chem.* **288,** 36538–36547 (2013).

54. Herrera, C., Tremblay, J. M., Shoemaker, C. B. & Mantis, N. J. Mechanisms of ricin toxin neutralization revealed through engineered homodimeric and heterodimeric camelid antibodies. *J. Biol. Chem.* **290,** 27880–27889 (2015).

55. Baty, Daniel; Chames, Patrick; Kerfelec,Brigitte; Turini, M. Anti-HER2 single domain antibodies, polypeptides comprising thereof and their use for treating cancer. 40 (2014).

56. Li, X. *et al.* Site-Specific Dual Antibody Conjugation via Engineered Cysteine and Selenocysteine Residues. *Bioconjug. Chem.* **26,** 2243–8 (2015).

57. Hober, S., Nord, K. & Linhult, M. Protein A chromatography for antibody purification.

Journal of Chromatography B: Analytical Technologies in the Biomedical and Life Sciences **848,** 40–47 (2007).

58. Lowe, E. S. & Balis, F. M. in *Principles of Clinical Pharmacology* 289–300 (2007). doi:10.1016/B978-012369417-1/50058-4
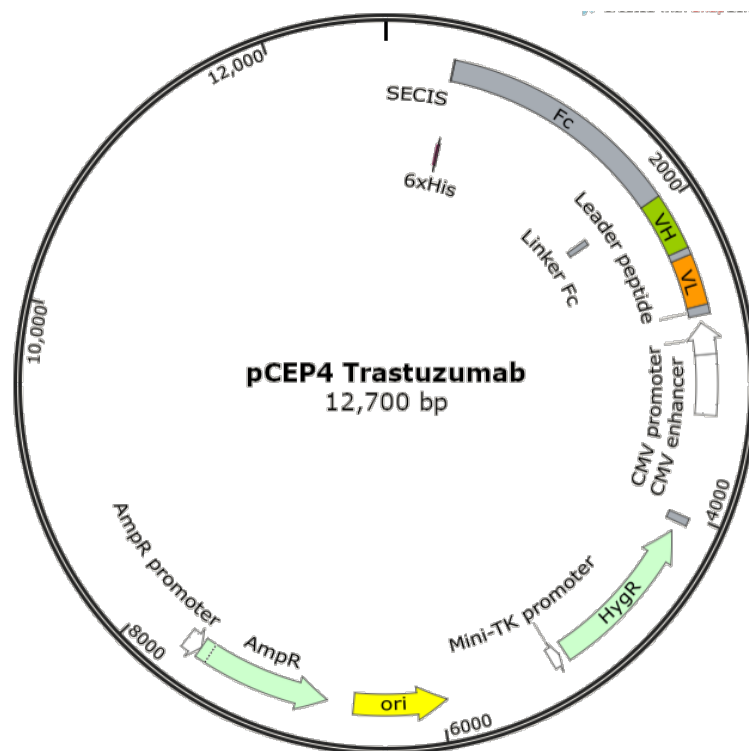
7.   Annexes

7.1   Bacteria Genotypes

<u>XL-1 Blue</u> - *recA1 endA1 gyrA96 thi-1 hsdR17 supE44 relA1 lac* [F´ *proAB lacI^qZ∆M15* Tn*10* (Tet^r)]

<u>JM109</u> - F´ *traD36 proA^+B^+ lacI^q Δ(lacZ)M15/ Δ(lac-proAB) glnV44 e14^- gyrA96 recA1 relA1 endA1 thi hsdR17*

7.2   Plasmid Maps
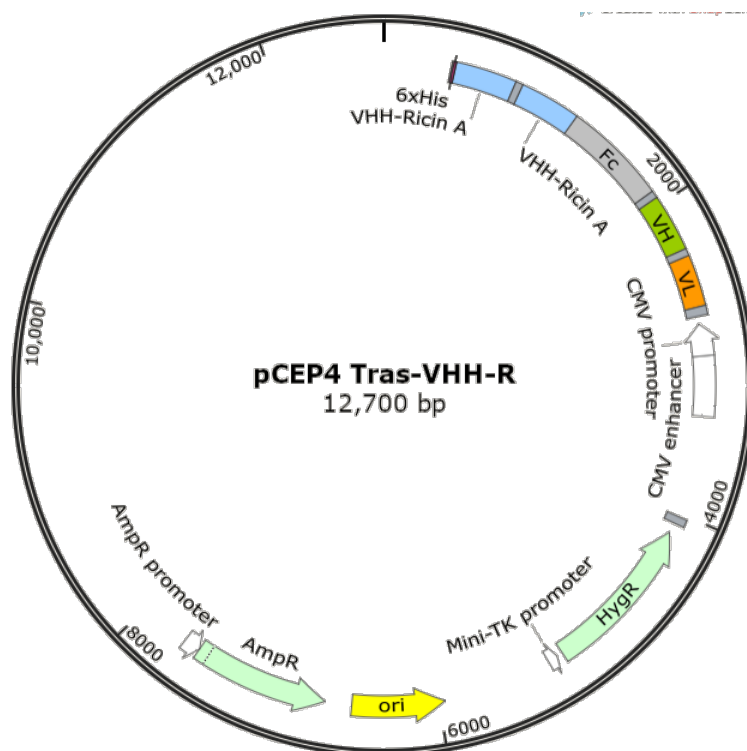

Figure 28 Plasmid map of pCEP4-Trastuzumab.
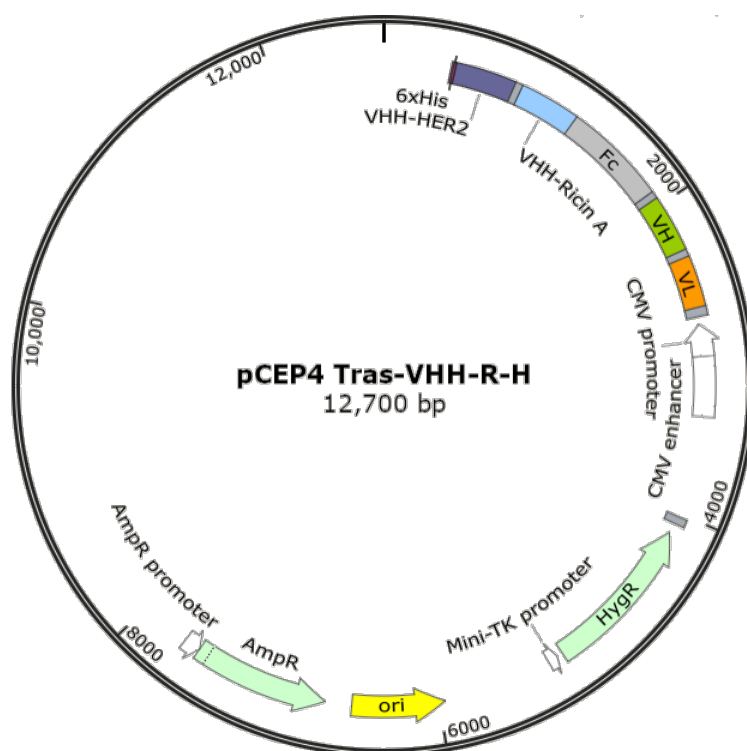
Figure 29 Plasmid map of pCEP4-VHH-R.

Figure 30 Plasmid map of pCEP4-VHH-R-H.

Universidade de Lisboa; Faculdade de Farmácia
Master in Biopharmaceutical Sciences

7.3 Absorbance of Purification Fractions

Table 2 Fractions absorbance at 280_{nm} from Trastuzumab purification by protein A affinity chromatography.

Trastuzumab Purification	
Fraction	A_{280nm} (1 Absorbance = 1mg/mL)
1	0,61
2	0,04
3	0,01
5	0,00
6	0,00
7	0,03
8	0,08
9	1,49
10	1,22
11	0,29
12	0,07
13	0,01
14	0,00
15	0,00
16	0,00
17	0,00
18	0,00
19	0,00
20	0,00
21	0,00
22	0,00
23	0,00

Table 3 Fractions absorbance at 280_{nm} from Tras-VHH-R purification by protein A affinity chromatography.

Tras-VHH-R Purification	
Fraction	A_{280nm} (1 Absorbance = 1mg/mL)
1	0,69
2	0,03
3	0,00
5	0,00
6	0,00
7	0,00
8	0,01
9	0,02
10	0,00
11	0,01
12	0,00
13	0,00
14	0,00
15	0,17
16	1,37
17	1,16
18	0,58
19	0,28
20	0,13
21	0,06
22	0,03
23	0,00
24	0,05
25	0,04
26	0,03

Table 4 Fractions absorbance at 280_{nm} from Tras-VHH-R-H purification by protein A affinity chromatography.

Tras-VHH-R-H Purification	
Fraction	A_{280nm} (1 Absorbance = 1mg/mL)
1	0,47
3	0,01
4	0,00
5	0,00
23	0,00
24	0,00
26	0,17
27	0,02
28	0,00